

**OSTEOGENIC EFFECT OF OPTIMIZED MUSCLE STIMULATION  
EXERCISE AS A COUNTERMEASURE DURING HINDLIMB UNLOADING**

A Thesis

by

LINDSAY REBECCA SUMNER

Submitted to the Office of Graduate Studies of  
Texas A&M University  
in partial fulfillment of the requirements for the degree of

MASTER OF SCIENCE

August 2007

Major Subject: Mechanical Engineering

**OSTEOGENIC EFFECT OF OPTIMIZED MUSCLE STIMULATION  
EXERCISE AS A COUNTERMEASURE DURING HINDLIMB UNLOADING**

A Thesis

by

LINDSAY REBECCA SUMNER

Submitted to the Office of Graduate Studies of  
Texas A&M University  
in partial fulfillment of the requirements for the degree of

MASTER OF SCIENCE

Approved by:

Co-Chairs of Committee:	Harry A. Hogan Susan A. Bloomfield
Member of Committee:	Anastasia Muliana
Head of Department:	Dennis O'Neal

August 2007

Major Subject: Mechanical Engineering

## ABSTRACT

### Osteogenic Effect of Optimized Muscle Stimulation Exercise as a Countermeasure During Hindlimb Unloading. (August 2007)

Lindsay Rebecca Sumner, B.S., Texas A&M University

Co-Chairs of Advisory Committee: Dr. Harry A. Hogan  
Dr. Susan A. Bloomfield

Rats that undergo hindlimb unloading (HU) as a simulation for microgravity experience bone responses similar to that seen by astronauts in space flight. A recent study showed that a resistance exercise regimen mitigated bone loss because of disuse. Controlled muscle stimulation was applied to the lower left limb to produce eccentric muscle contractions. The recent study, which showed beneficial effects on bone, did not show mitigation of muscle loss. The purpose of this project is to determine the bone response to a modified stimulation protocol by optimizing parameters to benefit bone and muscle.

Forty-six 5.5-month-old male rats were divided into 4 groups: baseline control (BC), cage control (CC), hindlimb unloaded no exercise (HU), and hindlimb unloaded with exercise (HU+Ex). Hindlimb unloading was achieved by tail suspension. The left leg of the HU+Ex group was exercised every other day for 28 days. The right leg of the HU+Ex group and the HU group served as disuse controls. The previous protocol consisted of 4 sets of 10 contractions, with 500ms stimulations, while the current protocol uses 4 sets of 5 repetitions at 1s stimulations. Eccentric contraction strength was changed from 120% peak isometric torque to 100%. Mechanical properties of the bone were measured at the proximal tibia metaphysis by using reduced platen compression (RPC) testing, directly loading only the cancellous compartment.

Results show ultimate stress levels in the HU+Ex group that are dramatically higher than HU values (+368%) and CC values (+275%), compared to 215% and no difference, respectively, for Alcorn's study. Ultimate stress values in HU and CC were not significantly different. The elastic modulus for the HU+Ex group tended to be 26% higher than that of the HU group, but was not statistically significant. The volumetric bone mineral density (vBMD) for HU+Ex was significantly higher than HU at the tibial

metaphysis (+16.8%), as compared to 11% in the previous study (Alcorn). Also, the vBMD for HU+Ex was greater than HU at the tibial midshaft (7%) after 28 days of unloading. These results show that the countermeasure effectively mitigated bone degradation induced by hindlimb unloading.

## TABLE OF CONTENTS

	Page
ABSTRACT.....	iii
TABLE OF CONTENTS .....	v
LIST OF FIGURES.....	vii
LIST OF TABLES .....	ix
LIST OF EQUATIONS.....	x
1. INTRODUCTION.....	1
1.1 Problem .....	1
1.2 Objectives .....	1
2. BACKGROUND.....	3
2.1 Bone structure.....	3
2.2 Steps of bone remodeling .....	3
2.3 Bone degenerative effects of exposure to microgravity in humans.....	5
2.4 Hindlimb unloading versus space flight in rats .....	6
2.5 Bone degeneration caused by disuse is attenuated by weight-bearing exercise.....	7
2.6 Osteogenic loading methods.....	8
2.6.1 Four-point bending .....	8
2.6.2 Ulna loader.....	9
2.6.3 Electric muscle stimulation.....	10
2.7 Compression testing for trabecular bone.....	12
3. EXPERIMENTAL METHODS.....	13
3.1 General overview .....	13
3.2 Experimental outline .....	13
3.3 Electrical stimulation protocol.....	15
3.4 pQCT procedure .....	17
3.5 Bone removal and preservation .....	19
3.6 Reduced platen compression testing.....	19
3.7 Statistical analysis.....	23
4. RESULTS .....	25
4.1 Introduction .....	25
4.2 Body weights .....	25
4.3 Tibial metaphysis bone mineral content (BMC) .....	26
4.3.1 Total BMC .....	26
4.3.2 Cancellous BMC .....	27
4.3.3 Cortical BMC .....	28
4.4. Tibial metaphysis areas .....	29

	Page
4.4.1 Total area .....	29
4.4.2 Marrow area .....	30
4.4.3 Cortical area .....	31
4.5 Tibial metaphysis volumetric bone mineral density (vBMD) .....	31
4.5.1 Total vBMD .....	31
4.5.2 Cancellous vBMD .....	33
4.5.3 Cortical vBMD .....	34
4.6 Tibial midshaft results .....	34
4.6.1 Midshaft total BMC .....	35
4.6.2 Midshaft cortical BMC .....	36
4.6.3 Midshaft total area .....	37
4.6.4 Midshaft cortical area .....	37
4.6.5 Midshaft marrow area .....	38
4.6.6 Midshaft total vBMD .....	39
4.6.7 Midshaft cortical vBMD .....	40
4.6.8 Midshaft cortical shell thickness .....	41
4.7 Mechanical properties .....	42
5. DISCUSSION .....	45
5.1 Purpose and general findings .....	45
5.2 Procedural caveats .....	46
5.2.1 Hindlimb suspension .....	46
5.2.2 Simulated resistive training via electrical muscle stimulation .....	47
5.2.3 Changes in material properties .....	48
5.2.4 Anesthesia control and weight loss .....	49
5.3 Comparison with previous HU+Exercise studies with rodents .....	49
5.3.1 Electric muscle stimulation of the free-hanging limb during HU ..	50
5.3.2 Voluntary flywheel exercise of HU rats .....	51
5.3.3 Limb immobilization, mechanical loading, and calcium restriction .....	51
5.3.4 Muscle stimulation simulated resistive exercise .....	53
5.4 Conclusion .....	55
6. FUTURE WORK .....	56
6.1 Potential muscle problems .....	56
6.2 Varying intensity levels .....	56
6.3 Drug and exercise interactions .....	56
REFERENCES .....	58
APPENDIX .....	62
VITA .....	67

## LIST OF FIGURES

	Page
Figure 1: Schematic representation of cancellous and cortical bone .....	3
Figure 2: Steps of bone remodeling .....	5
Figure 3: Diagram of a rat tibia undergoing four-point bending .....	8
Figure 4: Schematic of the ulna loader.....	9
Figure 5: Left (control) and right (loaded) ulnae demonstrate the increased bone formation during applied dynamic loading .....	10
Figure 6: Diagram of electric muscle stimulation unit.....	11
Figure 7: Example of the hindlimb suspended configuration.....	14
Figure 8: Schematic of the electric stimulation setup .....	15
Figure 9: Anesthetized rat undergoing the muscle stimulation protocol.....	16
Figure 10: (a) Schematic of stimulation set; (b) foot pedal configuration .....	17
Figure 11: Sample scout view of the tibia .....	18
Figure 12: Illustration of landmark and RPC specimen cutting location .....	20
Figure 13: Contact x-ray of an RPC sample.....	21
Figure 14: Sample radiograph with a superimposed endocortical circle .....	21
Figure 15: Schematic of RPC specimen and test.....	22
Figure 16: Body weights during 28 days of unloading .....	25
Figure 17: Total BMC of the tibial metaphysis during 28 days of unloading.....	26
Figure 18: Cancellous BMC of the tibial metaphysis during 28 days of unloading.....	27
Figure 19: Cortical BMC of the tibial metaphysis during 28 days of unloading.....	28
Figure 20: Total area of the tibial metaphysis during 28 days of unloading .....	28
Figure 21: Marrow area of the tibial metaphysis during 28 days of unloading.....	30
Figure 22: Cortical area of the tibial metaphysis during 28 days of unloading.....	31
Figure 23: Total vBMD of the tibial metaphysis during 28 days of unloading.....	32
Figure 24: Cancellous vBMD of the tibial metaphysis during 28 days of unloading.....	33
Figure 25: Cortical vBMD of the tibial metaphysis during 28 days of unloading.....	34
Figure 26: Total BMC of the tibial midshaft during 28 days of unloading.....	35
Figure 27: Cortical BMC of the tibial midshaft during 28 days of unloading .....	36
Figure 28: Total area of the tibial midshaft during 28 days of unloading.....	37

	Page
Figure 29: Cortical area of the tibial midshaft during 28 days of unloading.....	38
Figure 30: Marrow area of the tibial midshaft during 28 days of unloading.....	39
Figure 31: Total vBMD of the tibial midshaft during 28 days of unloading.....	40
Figure 32: Cortical vBMD of the tibial midshaft during 28 days of unloading .....	41
Figure 33: Cortical shell thickness of the tibial midshaft during 28 days of unloading..	42
Figure 34: Ultimate stress of the tibial metaphysis after 28 days of unloading.....	43
Figure 35: Elastic modulus of the tibial metaphysis after 28 days of unloading.....	44
Figure 36: Schematic illustration of in vivo 4-point bending.....	52
Figure 37: Comparison of foot pedal protocols for the study by Alcorn and the current study .....	54

**LIST OF TABLES**

	Page
Table 1: Summary of the tibial metaphysis pQCT results obtained at day 0 and day 28.....	62
Table 2: Summary of the tibial midshaft pQCT results obtained at day 0 and day 28 ...	63
Table 3: Summary of the mechanical testing data and body weights .....	63
Table 4: Number of animals per group.....	64
Table 5: Voltage (V) for peak isometric torque at 175 Hz.....	64
Table 6: Peak isometric torque at 175Hz.....	64
Table 7: Frequency needed for each 100% peak isometric torque .....	65
Table 8: Platen size for specimens .....	65
Table 9: Thickness for specimens .....	76

**LIST OF EQUATIONS**

	Page
Equation (1): Ultimate stress $\sigma_{ult}$ .....	23
Equation (2): Elastic modulus E .....	23

## 1. INTRODUCTION

### 1.1 Problem

The skeletal system adapts to changes in loading. Decreased loads, such as in microgravity or bed rest, can cause bone loss. These smaller loads cause the skeletal system to be less robust. Bone loss has been observed in Soviet cosmonauts on the space station MIR<sup>5</sup>. Members of the crew experienced an average loss in areal bone mineral density (BMD) of 0.8% per month, with 1.4% loss per month at the femoral neck. The average length of the space flight was 5.6 months. Urine calcium levels were seen to increase 33% after 84 days of space flight<sup>6</sup>. These observations indicate that maintaining bone mass is a concern when planning long term space flight.

Subjects exposed to long term microgravity may develop osteoporosis. Osteoporosis is defined by the World Health Organization as a BMD of 2.5 standard deviations or more below the young adult mean<sup>35</sup> and is characterized by low bone density, bone fragility, and increased fracture risk<sup>32</sup>. Weight bearing exercise has site-specific effects on loaded bone and the training stimulus must exceed loads seen during normal activity to have an impact on bone health<sup>4</sup>. In order for bone to have an osteogenic response to the exercise, the loads must be unique, variable, and dynamic<sup>31</sup>. A study that followed post-menopausal women observed a 0.4% increase in total body BMD over a 12-month period with weight-bearing exercise, with 1.2-2.1% increases in BMD at the femoral trochanter. While positive gains are incurred with high-intensity resistance exercise, these gains are not permanent and are only maintained by continued exercise<sup>31</sup>.

The mechanical integrity of the bone is characterized by its bone mineral density and geometry, and decreases during disuse<sup>30</sup>. The development of an anabolic exercise regimen may help attenuate bone loss due to disuse.

### 1.2 Objectives

Hindlimb unloading (HU) in rats is a ground-based model. It shows similar bone

---

This thesis follows the style of the Journal of Bone and Mineral Research.

responses as those in spaceflight and is frequently used as a model for humans in microgravity<sup>33</sup>. The purpose of this research is to evaluate the efficacy of a potential countermeasure for preventing (or mitigating) bone loss during unloading. The exercise countermeasure protocol consists of simulated resistive exercise of the hind limbs by using high force contractions<sup>34</sup>. The primary region of interest for evaluating bone loss is the proximal tibia, which is composed largely of cancellous bone. Previous studies have shown that microgravity causes more losses in the cancellous regions than in cortical bone<sup>12,21</sup>.

The effects of the countermeasure on bone properties using the HU rat animal model will be assessed in two ways. Firstly, volumetric bone mineral density (vBMD) of the proximal tibia and tibial midshaft will be measured by peripheral quantitative computed tomography (pQCT). Secondly, mechanical properties will be assessed by reduced platen compression (RPC) testing of cancellous bone from the proximal tibia metaphysis.

In previous studies, pQCT analysis of HU animals showed the total vBMD at the proximal tibia at 21 days to be lower than the cage control (CC) at 28 days<sup>21</sup>. However, a muscle stimulation countermeasure in hindlimb unloading showed that the simulated exercise induced higher total vBMD levels in the stimulated leg (11% greater) than the contralateral limb that did not receive stimulation<sup>19</sup>. In addition, the ultimate strength and elastic modulus for the exercised bone were higher than the non-exercised bone (by 68% and 81%, respectively). Hence, simulated resistance training exerted a positive effect on proximal tibia bone when compared to control and HU non-stimulated cases. Both the current study and the previous study by Alcorn<sup>19</sup> are part of a broader project examining both bone and muscle response to the simulated resistive exercise. Unpublished data from Alcorn's study indicated no beneficial effect of the exercise on muscle, despite the dramatic positive effects on bone. Hence, the muscle stimulation protocol parameters in the current study have been modified from those of the previous study<sup>19</sup> with the goal of optimizing the benefits such that the exercise mitigates negative effects of HU on both bone and muscle. The quantitative assessment of the material properties coupled with bone density data provide a comprehensive view of bone properties with this modified protocol.

## 2. BACKGROUND

### 2.1 Bone structure

The skeletal structure provides protection for the body's internal organs, as well as supports the body's load. The bones of interest in this study are the long bones that transfer load; these bones are most susceptible to fractures resulting from osteoporosis at mixed bone sites (i.e. the metaphyseal locations). The long bone metaphyses consist of an outer cortical shell and an inner trabecular or cancellous bone matrix. The cancellous (or "spongy") bone is found at the bulbous ends, while the shafts consist of mostly cortical ("hard") bone. The wide ends of the long bones help to distribute the transmitted load<sup>1</sup>, and the cancellous matrix acts as a shock absorber. Cortical bone makes up approximately 80% of the body's skeletal mass and serves as the main support of the skeletal system<sup>2</sup>. Figure 1 displays a schematic representation of human cortical and cancellous bone, including their respective locations in the long bones.

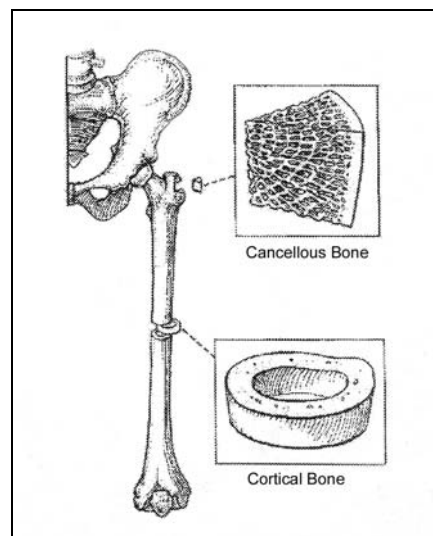


Figure 1: Schematic representation of cancellous and cortical bone<sup>3</sup>.

### 2.2 Steps of bone remodeling

Bone remodeling maintains a healthy bone structure by removing old bone and replacing it with new, and by adapting to mechanical loads to increase strength and stability. Bone removal is called resorption, and the process of forming new bone is

called formation. The average adult cortical bone has a life span of about 20 years, and cancellous bone lasts from one to four years<sup>2</sup>.

The process of bone formation and resorption is made possible by a group of cells (osteoclasts, which resorb bone, and osteoblasts, which build bone) combined into one unit called the basic multicellular unit (BMU). These units perform remodeling on cortical bone surfaces and on cancellous bone surfaces.

The three main phases of remodeling are activation, resorption, and formation, known as ARF. The total remodeling process in humans is approximately four months<sup>4</sup>. The ARF sequence can be broken down into six more defined sections: resting, activation, resorption, reversal, formation, and back to resting.

During the resting phase, the bone cells are inactive. Activation is initiated by a mechanical or chemical signal. The cells that rest on the bone surface digest the endosteal membrane and expose the bone underneath to osteoclastic cells. The resorptive phase brings the osteoclasts up to the exposed bone surface, allowing them to erode the bone and create cavities. During reversal, osteoclastic activity diminishes while the presence of osteoblasts increases. The following stage of bone formation is composed of matrix synthesis and mineralization. The new osteoblasts put down a layer of new bone matrix in the cavities created by the osteoclasts. This new matrix takes three to six months to completely mineralize<sup>2</sup>. The osteoblasts become osteocytes (bone cells), bone lining cells, or disappear as the final phase of resting begins. The process of remodeling is illustrated in Figure 2.

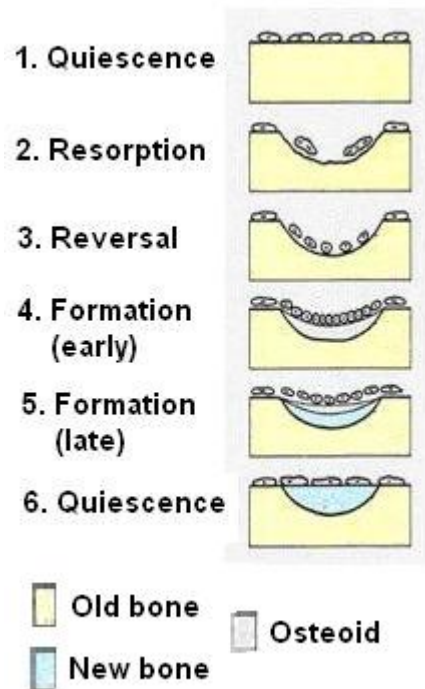


Figure 2: Steps of bone remodeling<sup>37</sup>.

### 2.3 Bone degenerative effects of exposure to microgravity in humans

The human skeletal system is a dynamic organ, adapting to its environment. It responds to many stimuli. One important environment and stimulus is long-term exposure to microgravity. Due to decreased loading on the skeletal structure, the bone adapts and becomes less robust, demonstrating the responsiveness to environmental changes. The trabeculae in mixed bone sites are aligned with the direction of the principle stresses of usual loading. When the loading patterns change, the bone reconfigures itself to adjust accordingly to meet the new strength requirements.

Skeletal deterioration has been observed at varying levels in astronauts and cosmonauts. For members of International Space Station (ISS) missions, bone loss at the femoral neck and total femur was found to be 1.5% per month, using DXA scans of bone mineral content (BMC)<sup>5</sup>. There was a significant increase in the blood calcium levels of cosmonauts after 114 days of space flight, as well as elevated levels of osteocalcin, an indicator of bone resorption<sup>6</sup>. These studies have shown that maintaining bone mass in microgravity is a challenge yet to be overcome. However, the results come from a small sample size and include inconsistencies between studies, such as differences in nutritional

intake, exercise exposure, and mission duration, that make it difficult to form conclusions.

#### **2.4 Hindlimb unloading versus space flight in rats**

Hindlimb suspension of rats has been developed as a model of microgravity similar to the “head-down” positioning of bed rest studies in human subjects. This positioning causes cephalic fluid shifts similar to those seen during space flight, and allows the rat normal mobility on its front limbs while removing weight-bearing forces from the hind limbs.

During hindlimb unloading in skeletally mature rats (six months old), bone formation dropped by nearly 80% in the tibial metaphysis and tibial midshaft in HU rats compared to pair-fed controls over a course of two and four weeks<sup>8</sup>. After one week of unloading, the surface area of cancellous bone occupied by osteoblasts was 66% lower than in the controls, indicating a decrease in bone formation. The cancellous bone volume, however, was unaffected, as was the surface area covered by osteoclasts on the trabeculae.

A hindlimb unloading study was performed comparing changes in bone in the hindlimb unloaded model versus that of spaceflown rats (3.5 months old)<sup>7</sup>. While both the HU animals and the animals in spaceflight lost bone volume (bone volume per total volume, or BV/TV), the spaceflown rats showed a greater loss of bone (55%) than the HU rats (29%) over a seven day period. There was a much greater decrease in trabecular density (55%) and increase in spacing (140%) in the spaceflight rats as compared to the HU group (~0% change for density and spacing). The change in trabecular thickness was the same between the two groups (25% decrease). The number of osteoclasts was increased by 113% in the suspended group, while there was no significant change in the spaceflight group.

While there are many similarities between hindlimb unloading and spaceflight, the HU model is not a perfect representation of zero gravity. In HU the forelimbs of the rats are resting on the ground, whereas in space the whole animal is floating. Also, the earthbound rats do not undergo the same stress levels experienced during reentry or the

delayed sacrifice, which introduces a short period of loading between landing and necropsy.

## **2.5 Bone degeneration caused by disuse is attenuated by weight-bearing exercise**

Exercise may prove to mitigate bone loss in a non-weight bearing setting. Julius Wolff noted that trabeculae align themselves in the direction of applied principal stresses. He suggested that the trabeculae respond to alterations in mechanical loading directions and orient themselves accordingly<sup>9,10</sup>.

Bedrest models have been used as a simulation of the microgravity experienced in space. During 17 weeks of bedrest, healthy males experienced bone loss in several key areas, including the lumbar spine (-3.9% change from baseline), femoral neck (-3.6%), and tibia (-2.2%), with a total body bone mineral loss of 1.4%<sup>11</sup>. In order to help mitigate bone loss, a resistance exercise countermeasure was employed during a 17-week period of bedrest. The group that was exposed to the exercise regimen experienced a 3.4% increase in lumbar spine BMD as compared to baseline values, -0.9% decrease in the total hip, and a 0.1% increase in the total body. These values were all significantly different from the control (no exercise) group, indicating that the exercise was beneficial in mitigating (and in some areas, preventing) bone loss<sup>12</sup>.

Rats that experienced hindlimb unloading as a disuse model exhibited a 45% decrease in mineral apposition rate (MAR), and suppression of bone formation rate per bone volume (BFR/BV) (-72%), as compared to long-term cage controls<sup>13</sup>. The HU group that underwent 10 minutes per day of mechanical intervention (low magnitude vibrating plate at 90Hz, 0.25g loading) showed attenuation of MAR and BFR/BV values in comparison to control values. The MAR was 1% below the control, and BFR/BV experienced a drop of 7%.

The incorporation of an anabolic exercise regimen into unloading can attenuate losses in rats, and may result in increases in human BMD at the lumbar spine and hip<sup>12</sup>.

## 2.6 Osteogenic loading methods

In vivo bone deformation is achieved in a variety of ways. Some methods are more physiological than others (i.e., apply loads in an approximately equivalent manner to normal ambulatory loading). Each of these approaches is useful in its own way in measuring bone strength and mechanical properties.

### 2.6.1 Four-point bending

*In vivo* loading using a four-point bending method has been shown to stimulate bone formation in rat tibia<sup>14</sup>. Loading is applied to the tibia so that the lateral side of the bone is in compression, and the anteromedial side is in tension, as demonstrated in Figure 3. Loading is applied at a rate of 2Hz and at varying cycles per day (from 1 to 108) for 12 consecutive days. The peak force applied is 37N. Bone formation increases as the number of loading cycles increases, and is observed to be greatest in the areas of the largest strain magnitudes (region A in Figure 3). These areas were within the 11mm section between the lateral loading points. Young's moduli were also measured in four-point in vitro bending and found to agree with previously reported results<sup>15</sup>.

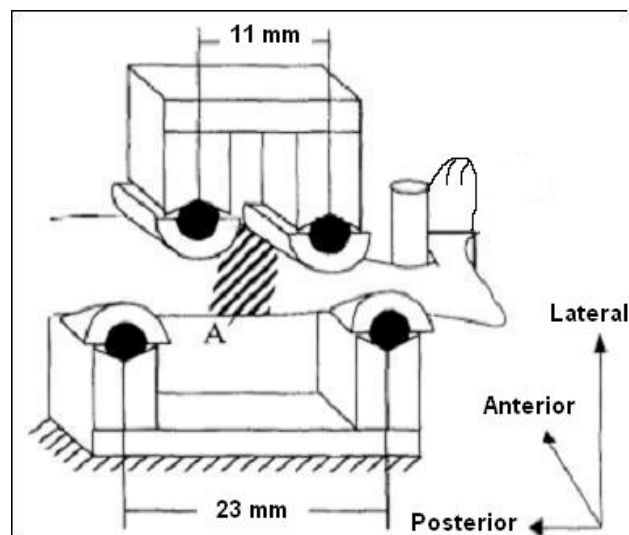


Figure 3: Diagram of a rat tibia undergoing four-point bending. The lateral surfaces are in tension from the lower (23mm) supports, while the medial surfaces undergo compression resulting from the downward force of the upper (11mm) supports. Region A indicates the area of highest strain magnitudes.<sup>14</sup>

### 2.6.2 Ulna loader

The ulna loader creates axial loads that are considered to be more mechanically appropriate than other loading methods, such as four-point bending. It applies loads through the olecranon and flexed carpus (Figure 4), and causes bending in the midshaft. This mode of loading induces strains that are above physiological exercise levels in rats.

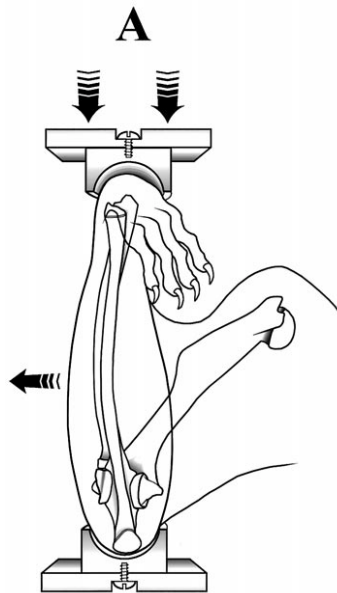


Figure 4: Schematic of the ulna loader.<sup>16</sup>

Cyclic loading of 1200 cycles was applied to the right ulna at 17 N, with loading occurring on days 1-5 and 8-12 of the study. This load level induced compressive strain levels of approximately  $3500\mu\epsilon$  on the medial surface of the ulnar midshaft<sup>16</sup>. The left limb served as a contra-lateral control. Results of the loading protocol showed a 78% increase in bone formation rate (BFR/BS) and a 67% increase mineral apposition rate (MAR) for the loaded bone as compared to the contra-lateral control. Figure 5 shows the increased bone formation surface for the loaded ulna.

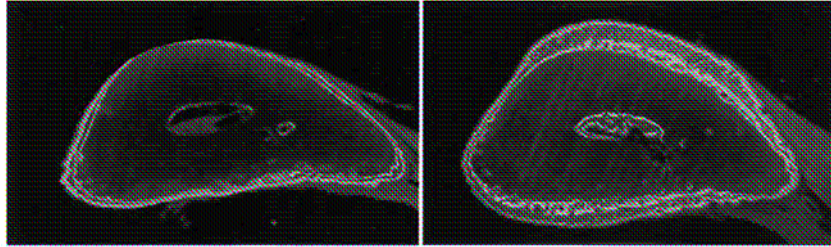


Figure 5: Left (control) and right (loaded) ulnae demonstrate the increased bone formation during applied dynamic loading.<sup>16</sup> The thick perimeter of the loaded ulna indicates newly formed bone.

The bending loads induced by loading of the ulna are not entirely physiological, however, because natural loading produces different strain levels and in different loading directions. In addition, normal ambulatory loading does not incur bending as seen in the ulna loader configuration. Loading using the animal's muscles could possibly induce a more physiological loading regime.

### 2.6.3 Electric muscle stimulation

*In vivo* loading of bone may be more physiological when applied using muscle acting on the bone in question. Electric muscle stimulation provides loading of the bone by stimulating the muscles, causing contractions and applying a physiological load on the bone. A schematic of the stimulation configuration can be seen in Figure 6. Stimulation is achieved by inserting fine wires on either side of the sciatic nerve and applying a voltage that induces a contraction. The foot is strapped to the pedal of the servo motor at a 90° angle with the lower leg, and the knee is clamped such that the tibia is at a 90° angle to the femur. The servo motor measures the torque exerted by the calf muscles on the ankle during contractions.

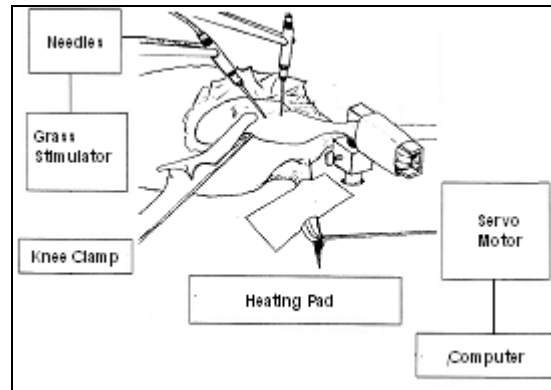


Figure 6: Diagram of electric muscle stimulation unit.

A previous study involving electric muscle stimulation in ovariectomized mice performed training using eccentric contractions of  $\sim 150\%$  of the peak isometric torque<sup>17</sup>. The training consisted of three sets of 10 eccentric contractions, performed every third day for eight weeks. The results of the mechanical testing (three-point bending) showed a significant increase in tibial stiffness for the trained group as compared to non-trained and control groups, but no changes in ultimate load. This is evidence that, while this study did not have markedly significant effects on bone, *in vivo* physiological loading using muscle stimulation has the potential to increase bone mechanical properties in situations that cause bone loss (i.e. unloading or estrogen deficiency).

A recent study done by the investigator's research group demonstrated significant improvements in bone mechanical properties during HU using electric muscle stimulation of the left leg<sup>19</sup>. The elastic modulus of the untrained right leg was 81% lower than that of the stimulated left leg, and 79% lower than the control group mean values. The trained leg in HU rats and the weight-bearing leg of the control group were not different, indicating that the training mimicked physiological levels of activity. Similarly, the ultimate stress for the no-exercise group was significantly lower than both the exercise group and the cage control, but there was no statistical significance between the values for the exercise group and the control group.

## 2.7 Compression testing for trabecular bone

There is a desire to be able to predict bone mechanical properties from non-invasive procedures, such as CT scanning. Correlations have been demonstrated between the elastic modulus of bone and apparent density<sup>18</sup>. However, when trying to predict mechanical properties directly from BMD, the difference between the calculated and measured values ranged from 40-60%. Based on these results, an accurate and reliable method of predicting mechanical properties has yet to be determined. To date, the most reliable method of determining bone mechanical properties is through *ex vivo* mechanical testing, due to the lack of relationship between imaging and mechanical properties. Such destructive testing methods as reduced platen compression (RPC) are useful for determining cancellous bone properties.

Because there is evidence that cancellous bone loss is much more significant than that of cortical bone in microgravity<sup>20,21</sup>, it is important to determine methods of measuring cancellous bone properties and identify modes of preventing loss. It is difficult to separate cortical bone properties from cancellous. This creates the need for a method to isolate the cancellous bone and measure its strength.

Reduced platen compression (RPC) is one such method of isolating the cancellous bone. A specimen obtained from the proximal tibia is placed between two platens of equal size and smaller in diameter than the cortical shell. Uni-axial compression is performed on the trabecular region without the platens touching any cortical bone. From the compression test, intrinsic bone properties can be calculated.

Platens of differing sizes are used because of the irregularity of bone geometry, caused by different ages and treatments between groups. The raw data from the compression test yields extrinsic properties that are only relevant to the specific specimen tested and do not give meaningful information about the bone. Intrinsic properties are obtained from manipulating the extrinsic data and normalizing for platen size so that comparison between specimens yields significant information concerning the quality and strength of the bone.

### 3. EXPERIMENTAL METHODS

#### 3.1 General overview

A general overview of the experimental procedure is described here. Detailed descriptions of the methods are provided in the following subsections. Mature male Sprague-Dawley rats were randomly assigned to four groups: baseline control (BC), cage control (CC), hindlimb unloaded no exercise (HU), and hindlimb unloaded with exercise (HU+ex). The length of the study was 28 days. BC represents measurements at day 0, and changes observed in CC rats demonstrate the effects of age and nutritionally related changes. The groups were normalized for body weight (BW) and vBMD, such that the average BW and vBMD for each group were not statistically different. The left leg of the HU+Ex group was stimulated every other day for the duration of the study. The right leg served as a contralateral control for the disuse model. In addition to this contralateral control, the HU group served as a disuse model as well as a comparison to the right leg of the HU+Ex group, to account for any differences caused by possible systemic responses in the exercise group that could affect the contralateral leg.

Bone density and cross sectional geometry of the proximal tibial metaphysis were assessed using peripheral quantitative computed tomography (pQCT) scans on days 0 and 28. The animals were sacrificed on day 28, and the tibias were extracted and frozen for later testing. Reduced platen compression (RPC) testing was performed on the tibial metaphysis to determine the mechanical properties (elastic modulus and ultimate stress) of the trabecular bone.

#### 3.2 Experimental outline

Forty-eight 5.5 month-old male Sprague-Dawley were divided into four groups and run in two cohorts of six rats in each of the following groups: BC, CC, HU, and HU+Ex. The body weights of the rats were measured using a Mettler PC 440 Balance (Mettler Instrument Corp, Hightstown, NJ). They were monitored daily and weighed weekly to detect any variation in weight over the course of the study. The pQCT scans of each rat's left leg measured the tibial metaphysis bone density prior to the study. The rats

were then stratified by total vBMD at the proximal tibia and randomly assigned to groups.

The animals were housed individually and maintained in an animal care facility at Texas A&M University that is accredited by the American Association for the Accreditation of Laboratory Animal Care. The housing room was maintained at a temperature of 72° F, with a 12:12 light/dark cycle.

The hindlimb suspension apparatus consisted of a U-shaped sling made of medical tape. The sling was attached, using marine glue, to the lateral sides of the rat's tail for three inches, starting about an inch above the base of the tail. At the end of the sling, a paper clip is attached, which then connects to an overhead wire. The animal is elevated approximately 30° so that the hind feet are just off the ground (Figure 7), but the rat is still able to move about the cage freely to groom, eat, and drink.

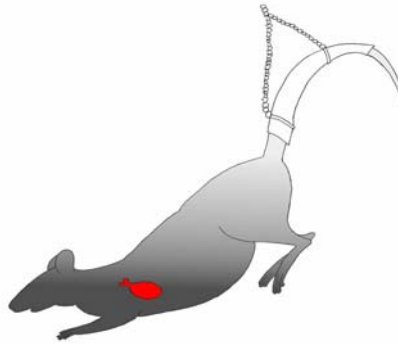


Figure 7: Example of the hindlimb suspended configuration.

The animals were fed standard Harlan Teklad 4% rodent chow (Teklad Premier, Madison, WI) for the duration of the 28-day study. All groups received food and water *ad libitum*. Baseline animals were sacrificed on day 0, and all others on day 28.

The left leg of the HU+Ex animals received electrical stimulation training every other day for the course of the study. This stimulation was intended to simulate resistance exercise. Proximal and midshaft tibial measurements were obtained at day 0 and day 28 using pQCT scans. Sacrifice occurred on day 28, and included tibial extraction, wrapping in saline-soaked gauze, and freezing at -80°C. RPC testing was

performed to determine mechanical properties of the proximal tibia cancellous bone, such as elastic modulus and ultimate strength.

### 3.3 Electrical stimulation protocol

The exercise protocol used in this study employed high-intensity eccentric muscle contractions as an exercise countermeasure. Others have demonstrated that as the intensity of mechanical loading increases, the number of loading cycles needed to create an osteogenic response decreases in mice<sup>39</sup>.

To run the protocol, the animal was anesthetized using isoflurane gas mixed with oxygen and maintained at a level that enabled full muscle function without consciousness of the animal. The rat was laid on its right side, and the foot was taped onto the footplate (Figure 8). The knee was clamped such that the shafts of the femur and tibia were at right angles to each other. The servo motor shaft was connected to the footplate and measured torque, displacement, and angle versus time during each contraction. Data was sampled at 10kHz. The Aurora Scientific 305B servomotor controller was used to synchronize the stimulation and contraction with the movement of the servo motor shaft, to which the footplate is attached. The Grass S48 stimulation unit and footplate rotation are controlled by custom software written in TestPoint software (courtesy of Gordon L. Warren III, Georgia State University).

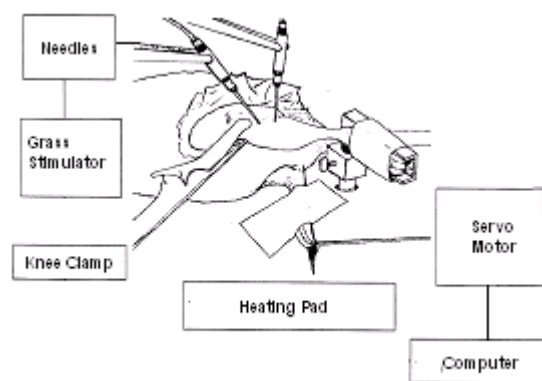


Figure 8: Schematic of the electric stimulation setup.

Electrical impulses are created using a Grass S48 stimulation unit. The stimulator control uses the following equipment: a 16 bit D/A and A/D board (KPCI-3108; Keithley

Insturments, Cleveland, Ohio, USA), an 866, a PC, and custom software written in Test Point (version 4.0; Capital Equipment Corp., Billerica, MA). The fine-wire stimulation probes are inserted on either side of the sciatic nerve (Figure 9). A voltage optimization (sweeping from 3 to 15 volts) is performed at the start of each exercise protocol to determine the peak isometric torque at 175Hz. An isometric contraction is defined as one in which the muscle does not stretch or contract, and an eccentric contraction describes a muscle that lengthens while it contracts. The simulated resistive exercise employed eccentric muscle contractions. The stimulation frequency was adjusted such that the torque during eccentric contraction is 100% of the peak isometric torque.

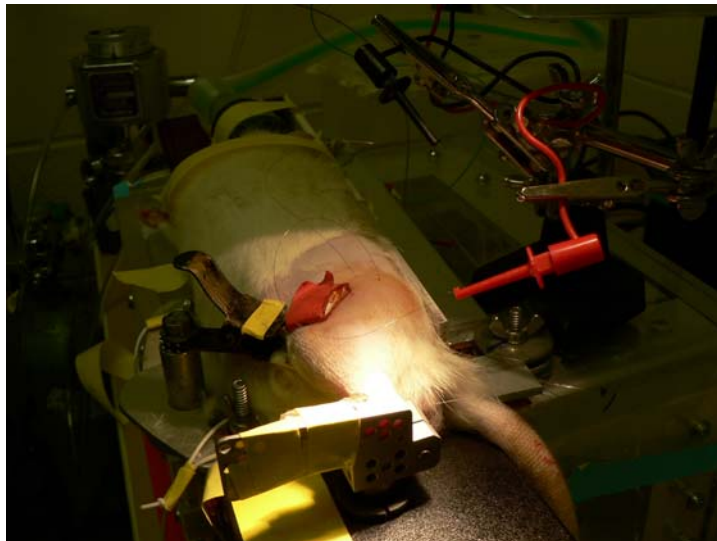


Figure 9: Anesthetized rat undergoing the muscle stimulation protocol (footplate in the foreground).

During the exercise procedure, the stimulation lasts for 1000ms (1s). The footplate to which the foot is secured is synchronized to rotate through 40 degrees during stimulation. It starts at 20° of dorsiflexion (relative to the 0° position of the foot) (Figure 10b). Just prior to muscle stimulation, the pedal rotates to the perpendicular position (Figure 10b, arrow 1), and the contraction begins. As the pedal rotates forty degrees (Figure 10b, arrow 2), producing dorsiflexion at an angular velocity of forty degrees per second, the muscle is simultaneously stimulated. This provides an eccentric contraction on the posterior crural muscle group of the lower leg. After the contraction, the foot and pedal return to the initial (20°) position (Figure 10b, arrow 3). The exercise regimen

consists of four sets of five repetitions (Figure 10a), with a contraction every twelve seconds and a two minute rest between sets, for a total of twenty contractions per day. The animals were subjected to the exercise regimen every other day for four weeks, yielding a total of fourteen exercise sessions.

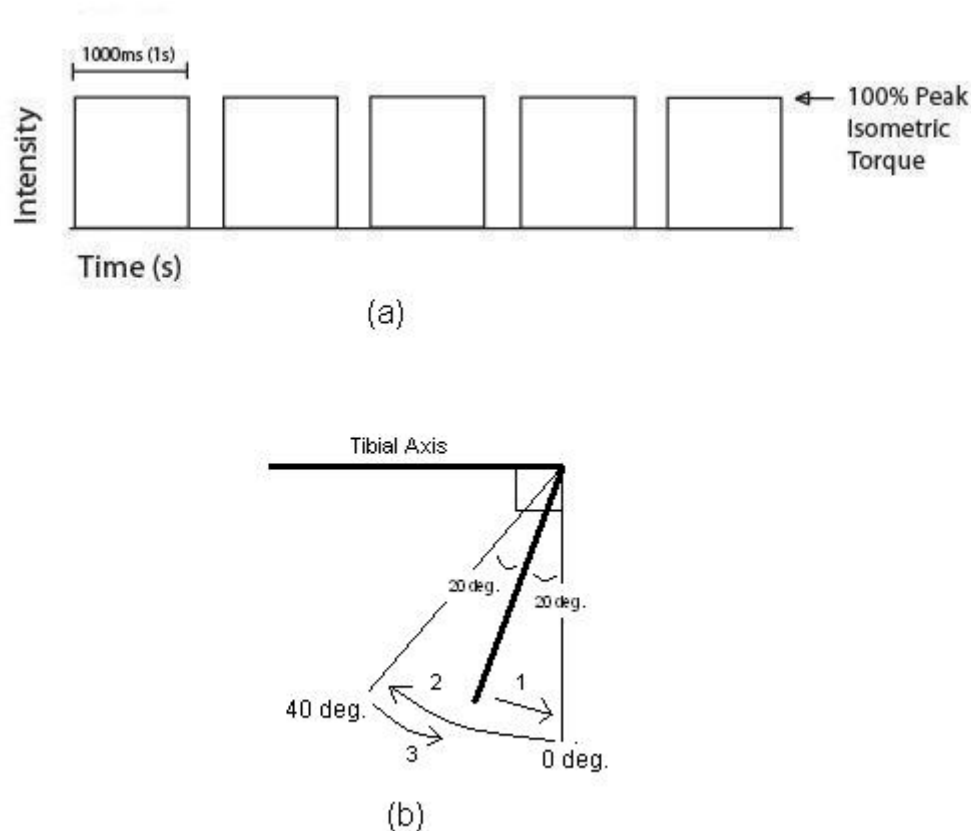


Figure 10: (a) Schematic of stimulation set; (b) foot pedal configuration.

### 3.4 pQCT procedure

Measurements of the tibial bone density were taken in vivo using a peripheral quantitative computed tomography (pQCT) device (Stratec XCT Research M; Norland Corp., Fort Atkinson, WI). The animals were anesthetized with a ketamine/medetomidine cocktail (1 mg/kg BW, given subcutaneously) and situated on the scanning platform with the left leg extended into the CT scanner gantry. The leg was taped securely to prevent movement. An initial scout view of the entire tibia was performed to verify correct positioning and to determine scan slice positions (Figure 11). A reference

line was placed at the proximal tibial plateau, and scan slices of the tibial metaphysis are collected at 5mm, 5.5mm, and 6mm from the tibial plateau. In addition, a slice of the distal tibial midshaft is measured at 50% of the total bone length. All slice thicknesses are 0.5mm. In order to accommodate the diameter of the leg, a scanning diameter of 45 mm is necessary, which requires a minimal voxel size of  $100\mu\text{m}$ . Total scan time takes 30 to 45 minutes from the start of the scout view to the end of the scanning. Once the scans have been completed, data from the three metaphyseal slices are averaged to get a single value for each variable.

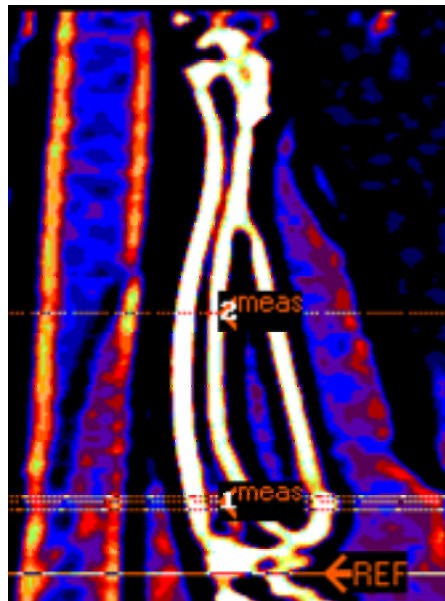


Figure 11: Sample scout view of the tibia. The reference line marks the tibial plateau. “1meas” indicates the placement for the metaphyseal scans, and “2 meas” indicates the midshaft scan location.

The cortical section of the bone consists of compact bone, while the cancellous section is comprised of “spongy” or trabecular bone. Important values obtained from the scans consist of the following: total, cortical, and cancellous volumetric bone mineral density (vBMD); total and cortical bone area; total bone mineral content (BMC); and cross-sectional moment of inertia (CSMI). “Total” indicates the entire amount of bone included in the scan. “Cortical” indicates the measurement of the cortical shell and does not include the marrow area or trabecular area. “Cancellous” describes the bone measurements in the area occupied by the trabeculae, or the marrow area. The marrow

area is defined as the region within the endocortical shell and contains the cancellous bone as well as the space between trabeculae. BMC is the amount of bone mineral present in a defined region of interest. vBMD is the BMC divided by the volume of bone in the three metaphyseal scans. CSMI indicates resistance to bending. Machine precision (based on manufacturer data) is  $\pm 3\text{mg/cm}^3$  for cancellous bone and  $\pm 9\text{mg/cm}^3$  for cortical bone. In vivo coefficients of variance from the investigator's laboratory using this method at the proximal tibia (with repositioning between scans) are  $\pm 2.19\%$  for cancellous vBMD,  $\pm 0.23\%$  for cortical vBMD, and  $\pm 1.95\%$  for total area. Corresponding CV's at mid-diaphysis for the tibia are  $\pm 0.36\%$  for cortical vBMD,  $\pm 1.09\%$  for cortical area, and  $\pm 2.42\%$  for marrow area<sup>21</sup>.

### **3.5 Bone removal and preservation**

Anesthetized animals were euthanized by decapitation, and all tibias were collected at necropsy. Each proximal tibia was cleaned of soft tissue, wrapped in gauze soaked in phosphate-buffered saline (Ringer's solution) for preservation, stored in plastic vials, and frozen at  $-80^\circ\text{F}$ . As noted in a study performed by Pelker (1984), freezing the bones does not significantly affect mechanical properties.

### **3.6 Reduced platen compression testing**

Reduced platen compression testing measures the strength of the cancellous bone in the metaphyseal region. Because cortical bone properties affect the mechanical properties of cancellous bone in whole bone testing, a method was developed to measure cancellous bone properties, with minimal effects from cortical bone<sup>22</sup>.

The proximal tibia was allowed to thaw to room temperature and thoroughly cleaned of any additional soft tissue. The epiphysis thickness (or distance from the tibial plateau to the growth plate) was measured three times and an average was taken. The end of the epiphysis (distal to the tibial plateau) is denoted by a "landmark" jutting of bone on the anterior side of the tibia (Figure 12). This marks the end of the growth plate, or where the growth plate and the proximal metaphysis meet indicated by "distance to growth plate" in Figure 12. The sample was mounted in plastic grippers, and the tibial plateau was aligned parallel to a Buehler Isomet low speed diamond wafer saw blade,

model 11-4244. The first cut was made based on the predetermined height of the epiphysis. Visual inspection of the specimen was also performed to ensure that the cut cleared the growth plate. To cut a 2mm sample, a 2.3mm distance was measured distally from this point, to account for the thickness of the saw blade (0.3mm). Once the sample was cut, the specimen height was measured using a digital caliper and recorded.

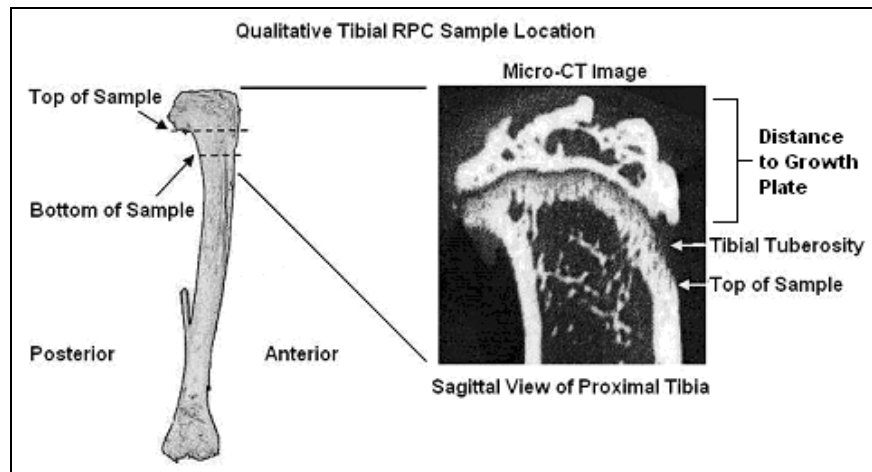


Figure 12: Illustration of landmark and RPC specimen cutting location.<sup>19</sup>

To determine the appropriate size of the platen for the compression test, the specimens were thawed to room temperature, placed proximal side down on x-ray film, and radiographed at 20 kV, 1 mA, and 70 seconds. These radiographs were used in determining platen size (Figure 13). Radiographs were radiated with a General Electric Industrial Radiograph Machine (General Electric, Lexington, MA) and developed on Kodak X-Omat TL Film (Eastman Kodak Company, Rochester, NY). The focal film distance was fixed at 30 inches. The radiographs were digitized using a Nikon Coolscan 5000, at 4000 dpi.

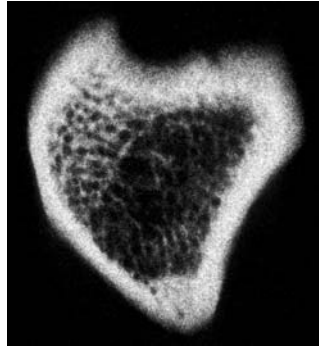


Figure 13: Contact x-ray of an RPC sample.

The scanned radiograph was viewed in Adobe Illustrator, and a circle was superimposed over the image to determine platen size (Figure 14). The circle should be as large as possible and just inscribing the endocortical perimeter. The platen size was determined by taking 70% of the diameter of the largest circle. The platen diameters are available in increments of 0.05mm. Visual inspection was performed by placing the platen against the specimen to determine a good fit and to make any necessary adjustments to the platen size.

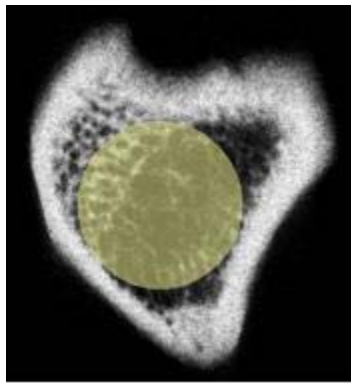


Figure 14: Sample radiograph with a superimposed endocortical circle.

On the day of the test, samples were thawed to room temperature, grouped from smallest to largest by platen size, and were tested in that order. To perform the test, the platens were fixed in an Instron model 1125, with a 1000lb load cell. The maximum range of the load cell for the test was set to 25 pounds. The specimen was placed between the two platens, and the upper platen was lowered until it barely touched the specimen. Quasi-static compression loading was applied at 0.51mm/min by lowering the upper platen, keeping the lower platen stationary (Figure 15). Displacement was

measured using a linear variable differential transformer (LVDT), calibrated to have a total stroke (or movement) of 0.05mm between -10 V and 10 V. Load and displacement data were collected digitally at a sampling rate of 10Hz using Labtech Notebook Pro Software Version 8.01 (Laboratory Technologies Corporation, Wilmington, MA) on a desktop PC.

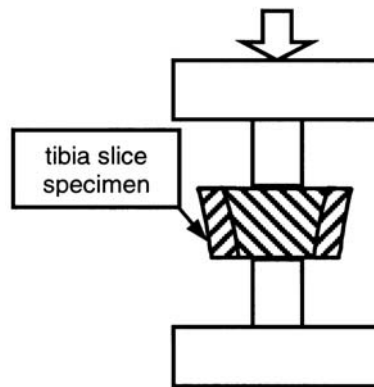


Figure 15: Schematic of RPC specimen and test.<sup>22</sup>

The raw data from the mechanical testing were recorded in pounds for force, inches for displacement, and seconds for time. Manipulation of this data yields results in Newtons, millimeters, and seconds for force, displacement, and time, respectively. From these converted data, the parameters of interest are further determined.

The testing was idealized to be uniaxial. Thus the volume of tested material can be computed from the specimen thickness ( $t$ ) and the cross-sectional area of the platen ( $A_{pl}$ ). The extrinsic parameters of interest collected from the force-displacement data are as follows:

- Maximum force ( $F_M$ ) in Newtons
- Displacement at maximum force ( $D_M$ ) in millimeters
- Stiffness ( $k$ ) in N/mm.

These parameters were determined using Microsoft Excel and TableCurve 2D (version 2.03; Jandel Scientific, San Rafael, CA). They represent the mechanical response of the structure and are dependent on size and shape of each specimen.

In a pure uniaxial state, the intrinsic properties were determined as follows:

- Ultimate stress ( $\sigma_{ult}$ ) is the strength of the material (in MPa) at maximum force and is defined by:

$$\sigma_{ult} = \frac{F_M}{A_{pl}} \quad (1)$$

where  $F_M$  is the maximum force, and  $A_{pl}$  is the cross-sectional area of the platen used to compress the trabecular structure.

- Elastic modulus ( $E$ ) is the stiffness (in MPa) of the trabecular bone structure when compressed and is defined by:

$$E = \frac{\sigma_{yy}}{\epsilon_{yy}} = \frac{F_M t}{\Delta t A_{pl}} = \frac{kt}{A_{pl}} \quad (2)$$

where  $k$  is the stiffness (from the linear portion of the force-displacement curve),  $t$  is the thickness of the specimen, and  $A_{pl}$  is the cross-sectional area of the platen.

The extrinsic properties from the raw data of the specimens cannot be compared due to the differences in geometric structure and varying platen sizes. The equations for the intrinsic properties normalize these values such that the calculated values provide meaningful comparisons of each sample's material properties.

### 3.7 Statistical analysis

The data will be reported in the form of mean  $\pm$  standard error in the graphs, and mean  $\pm$  standard deviation in the text and tables. The longitudinal pQCT data were analyzed using a two-way ANOVA with a pairwise Holm-Sidak comparison method. The first sorting factor was for the time, i.e. day 0 or day 28. The second was the treatment group to which each bone belonged, that is, HU+Ex, HU, and CC. The baseline (BC) group was excluded from this statistical analysis because its data is not longitudinal and only contains day 0 data, which can be obtained from cage control data at day 0. Comparisons among groups at day 28 were included in the two-way ANOVA.

Both the right and left tibias from all groups were collected, creating a right and left subgroup within each treatment group for the mechanical properties. For all groups except HU+Ex, a t-test was run between right and left to determine the animals' "handedness", or whether it favored a particular leg. Because much of the mechanical

testing data was not normally distributed, a Mann-Whitney Rank Sum test was performed. For the HU treatment group, the unexercised right leg of the HU+Ex group was included in the statistical analysis with the data from HU (both right and left legs) for the mechanical testing.

The statistical analysis of the mechanical properties was performed using a Kruskal-Wallis one-way ANOVA on ranks, because the data were not normally distributed. The one-way ANOVA analysis was used because the data were not longitudinal. That is, the mechanical tests can only be conducted at the endpoint for each animal because it requires an excised bone and is a destructive test. BC values were reported in the graphs as a reference point but were not included in the statistics because they were not of the same age as the other treatment groups. The data were organized into treatment groups: none (CC), HU, and HU+Ex. The comparison of HU and HU+Ex demonstrates the effectiveness of the exercise countermeasure to disuse. The comparison of HU and CC illustrates the change due to disuse.

## 4. RESULTS

### 4.1 Introduction

This section contains the results of the pQCT data, illustrating changes in vBMD, BMC, and tibial cross-sectional area. The intrinsic mechanical properties of tibial cancellous bone, as determined by RPC testing, are also presented in this section.

### 4.2 Body weights

For the groups in suspension (HU, HU+Ex), the body weight of the rats was found to be significantly lower ( $P < 0.001$ ) than the age-matched control (CC) after 28 days (Figure 16). In addition, the HU+Ex group showed significantly lower body weights than HU at day 28, with a 6.7% difference ( $P = 0.035$ ). The body weights of the HU+Ex group decreased significantly over the course of the study ( $388.25 \pm 14.80$  g vs.  $423.08 \pm 29.18$  g,  $P = 0.003$ ), while those of the HU group did not change. The CC body weights increased 11.3% between day 0 and day 28 ( $P = 0.003$ ). All groups were fed *ad libitum*.

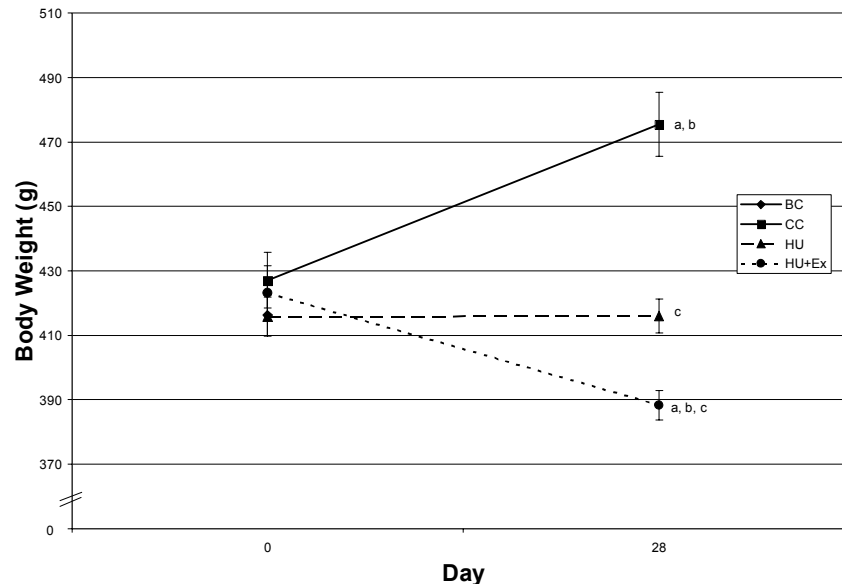


Figure 16: Body weights during 28 days of unloading. The left leg of HU+Ex received muscle contraction exercise. *a*:  $P < 0.05$  vs. HU values; *b*:  $P < 0.05$  vs. day 0 within group; *c*:  $P < 0.05$  vs. CC values.

### 4.3 Proximal tibial metaphysis bone mineral content (BMC)

All results from pQCT analyses at the proximal tibial metaphysis are summarized in Table 1 (p. 62). The following sections contain graphical presentations of the results along with brief explanations of statistical comparisons and results.

#### 4.3.1 Total BMC

Exercise as a countermeasure was found to have an effect on the total bone mineral content of the tibial metaphysis (Figure 17). BMC is reported because it is a measure of the total bone mineral present, allowing observations of actual changes to bone size. The total BMC of the HU+Ex group is 22% larger than that of HU at 28 days ( $12.46 \pm 0.54$  mg vs.  $10.22 \pm 0.53$  mg;  $P < 0.05$ ). The final value for total BMC in the HU+Ex group does not have any statistical difference from the control group ( $P = 0.865$ ). The HU group was 16% lower than CC at 28 days ( $12.17 \pm 1.08$  mg vs.  $10.22 \pm 0.53$  mg;  $P = 0.025$ )

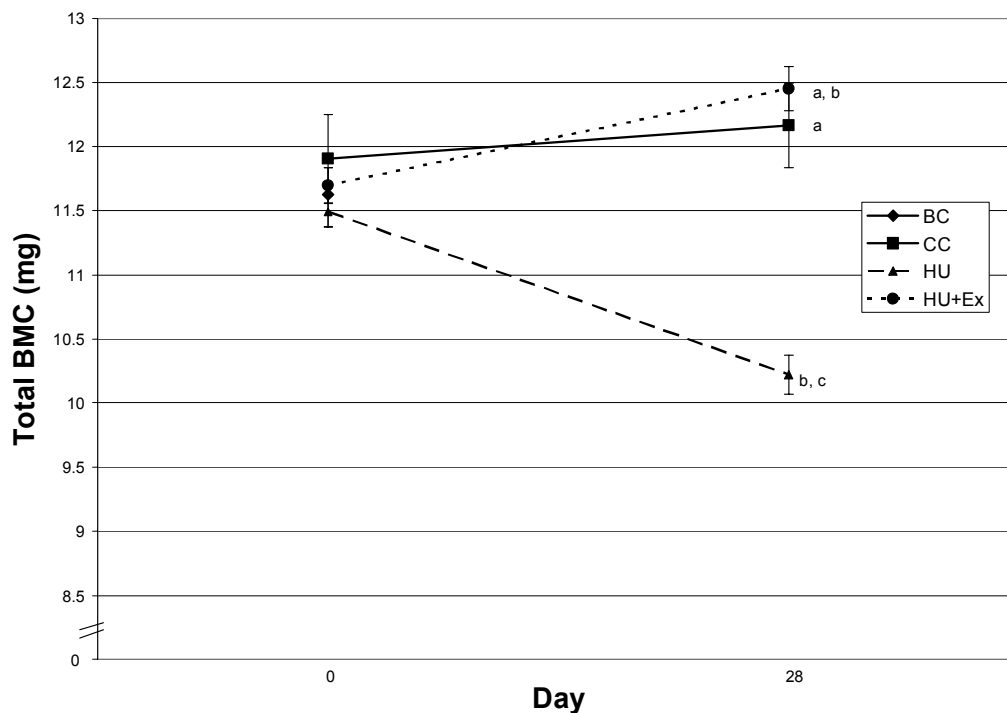


Figure 17: Total BMC of the tibial metaphysis during 28 days of unloading. The left leg of HU+Ex received muscle contraction exercise. *a*:  $P < 0.05$  vs. HU values; *b*:  $P < 0.05$  vs. day 0 within group; *c*:  $P < 0.05$  vs. CC values.

Two-way ANOVA shows a significant difference in values within groups for day 0 and day 28 measurements ( $P < 0.001$ ). The post hoc pairwise comparison of the HU+Ex group's values at day 28 vs. day 0 exhibited a 7% increase ( $P = 0.026$ ). The HU total BMC values showed an 11% decrease from day 0 ( $P = 0.05$ ). The control group did not significantly change over the 28 day period. The countermeasure maintained and increased the total BMC during disuse to a level greater than that of the cage control group after 28 days.

#### 4.3.2 Cancellous BMC

The countermeasure did not affect changes in the cancellous BMC when using a two-way ANOVA ( $P = 0.067$ ) (Figure 18). Comparisons at day 0 and day 28 did not show any differences among groups.

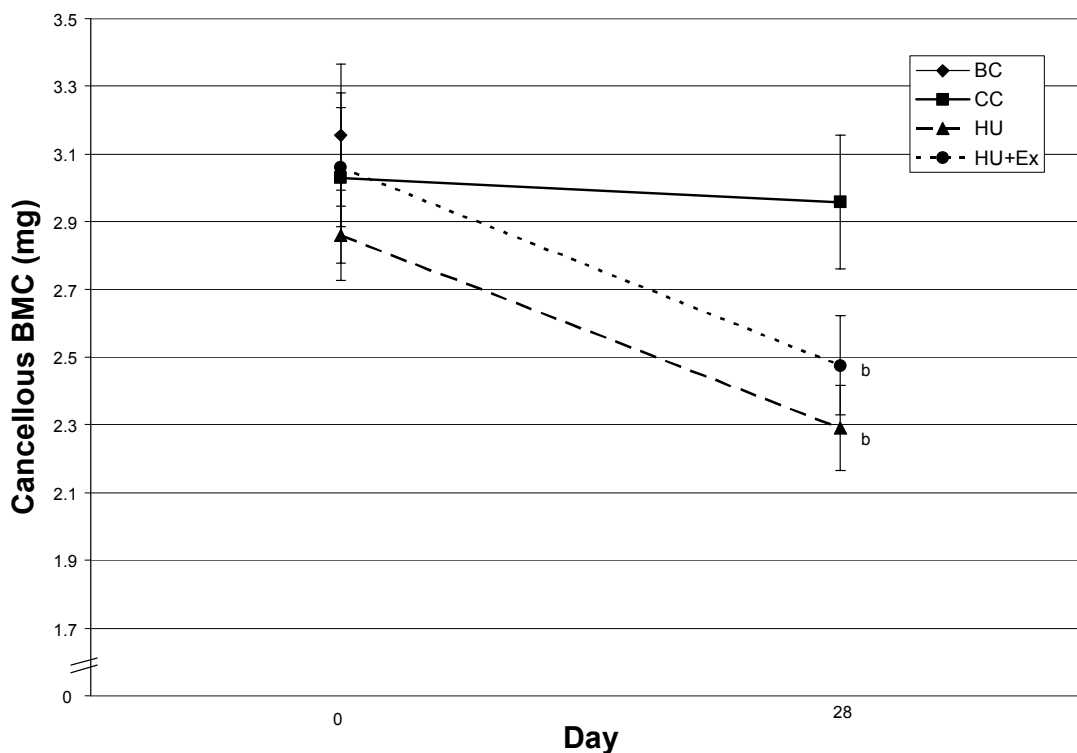


Figure 18: Cancellous BMC of the tibial metaphysis during 28 days of unloading. The left leg of HU+Ex received muscle contraction exercise. *b*:  $P < 0.05$  vs. day 0 within group.

Within treatment groups, post hoc pairwise comparisons showed significant differences over the course of time. Cancellous BMC in HU+Ex decreased 19% over the

28 day period ( $3.06 \pm 0.61$  mg to  $2.48 \pm 0.46$  mg,  $P < 0.05$ ). The measured values for HU decreased by 20% ( $2.86 \pm 0.46$  mg to  $2.29 \pm 0.43$  mg,  $P < 0.05$ ). The cage control's BMC did not change significantly.

#### 4.3.3 Cortical BMC

At the tibial metaphysis, the cortical BMC (Figure 19) of the HU+Ex group was 19.7% greater than the values for the HU group after 28 days ( $8.82 \pm 0.45$  mg vs.  $7.37 \pm 0.49$  mg,  $P < 0.001$ ), and 6.8% greater than CC ( $8.82 \pm 0.45$  mg vs.  $8.26 \pm 0.39$  mg,  $P = 0.006$ ). The CC was also 12.1% greater than HU at day 28 ( $8.26 \pm 0.39$  mg vs.  $7.37 \pm 0.49$  mg,  $P < 0.001$ ). The countermeasure was effective in mitigating loss of cortical BMC due to disuse and raised levels above that of the control group. There were no significant differences among groups at day 0.

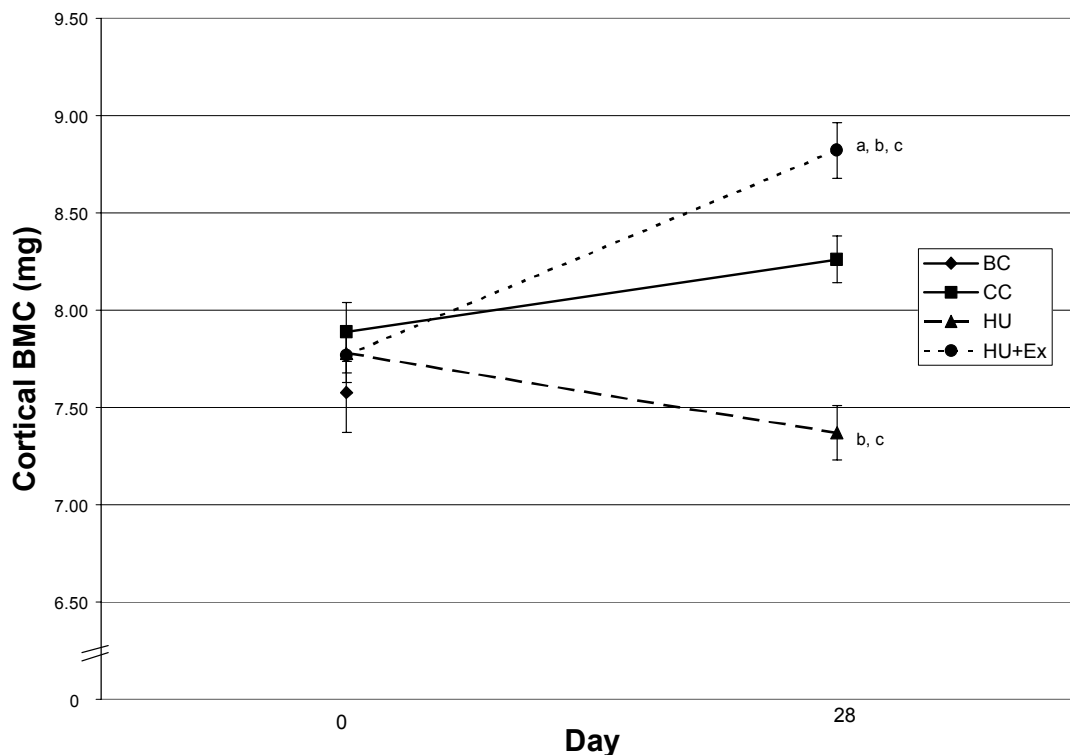


Figure 19: Cortical BMC of the tibial metaphysis during 28 days of unloading. The left leg of HU+Ex received muscle contraction exercise. *a*:  $P < 0.05$  vs. HU values; *b*:  $P < 0.05$  vs. day 0 within group; *c*:  $P < 0.05$  vs. CC values.

Post hoc comparisons of the groups showed a 13.5% increase in cortical BMC for the HU+Ex group over 28 days ( $8.82 \pm 0.45$  mg vs.  $7.77 \pm 0.49$  mg,  $P < 0.001$ ). The HU group significantly decreased 5.3% between day 0 and day 28 ( $7.37 \pm 0.49$  mg vs.  $7.78 \pm 0.35$  mg,  $P = 0.032$ ). The CC group did not significantly change. The countermeasure aided in abating cortical BMC loss during disuse.

#### 4.4 Tibial metaphysis areas

##### 4.4.1 Total area

The total cross-sectional area of the tibial metaphysis (Figure 20) for the HU+Ex group is 4% larger than HU after 28 days but is not statistically different ( $P = 0.227$ ). However, both groups were statistically smaller than the CC at day 28 ( $P < 0.01$ ). The HU+Ex mean area was 11.2% smaller than that of CC ( $18.31 \pm 0.79$  mm<sup>2</sup> vs.  $20.36 \pm 2.28$  mm<sup>2</sup>,  $P = 0.017$ ), and the area for HU was 15.6% smaller ( $17.61 \pm 1.33$  mm<sup>2</sup> vs.  $20.36 \pm 2.28$  mm<sup>2</sup>,  $P = 0.025$ ).

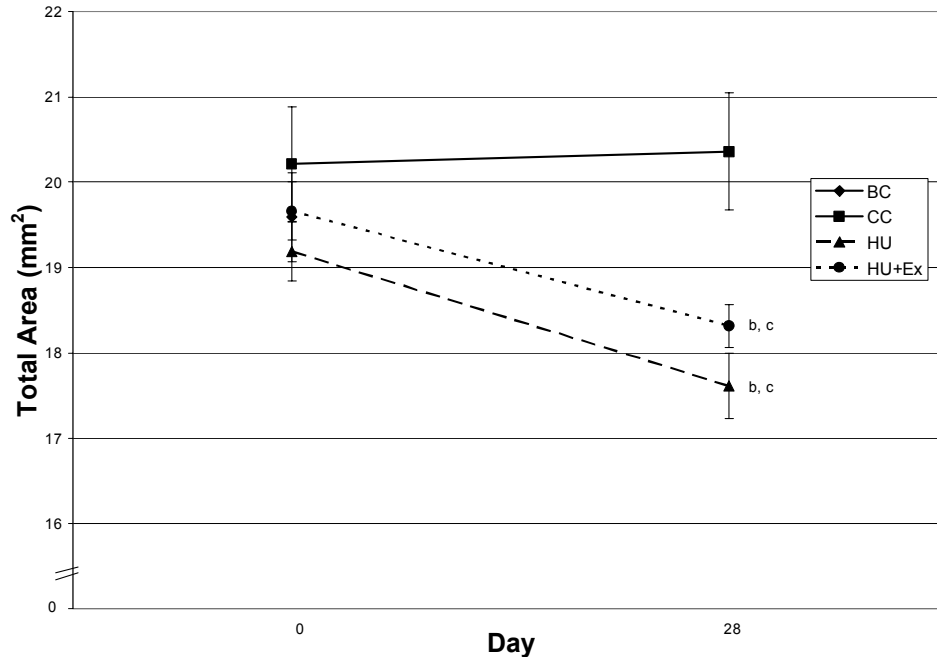


Figure 20: Total area of the tibial metaphysis during 28 days of unloading. The left leg of HU+Ex received muscle contraction exercise. *b*:  $P < 0.05$  vs. day 0 within group; *c*:  $P < 0.05$  vs. CC values.

Mean values at day 0 were not different. Both HU+Ex and HU showed decreases in areas over 28 days. Areas for HU+Ex declined 6.9% ( $18.31 \pm 0.79 \text{ mm}^2$  vs.  $19.66 \pm 1.18 \text{ mm}^2$ ,  $P=0.022$ ), and those of HU decreased 8.2% ( $17.61 \pm 1.33 \text{ mm}^2$  vs.  $19.19 \pm 1.19 \text{ mm}^2$ ,  $P=0.022$ ). The CC group's mean area did not significantly change over the course of the study.

#### 4.4.2 Marrow area

The cross-sectional marrow area (Figure 21) bounded by the endocortical surface of the tibial metaphysis for the HU+Ex group was 19% lower than the CC values after 28 days ( $9.30 \pm 0.73 \text{ mm}^2$  vs.  $11.56 \pm 1.79 \text{ mm}^2$ ,  $P=0.017$ ), and HU values were 12.2% lower than the cage control at day 28 ( $10.15 \pm 1.19 \text{ mm}^2$  vs.  $11.56 \pm 1.79 \text{ mm}^2$ ,  $P=0.025$ ). The CC and HU marrow areas did not change significantly from day 0 to day 28. The HU+Ex group showed a significant area decrease over the 28 day period (17.4%,  $P=0.001$ ). This change in marrow area may be a major contributor to the increase in total vBMD.

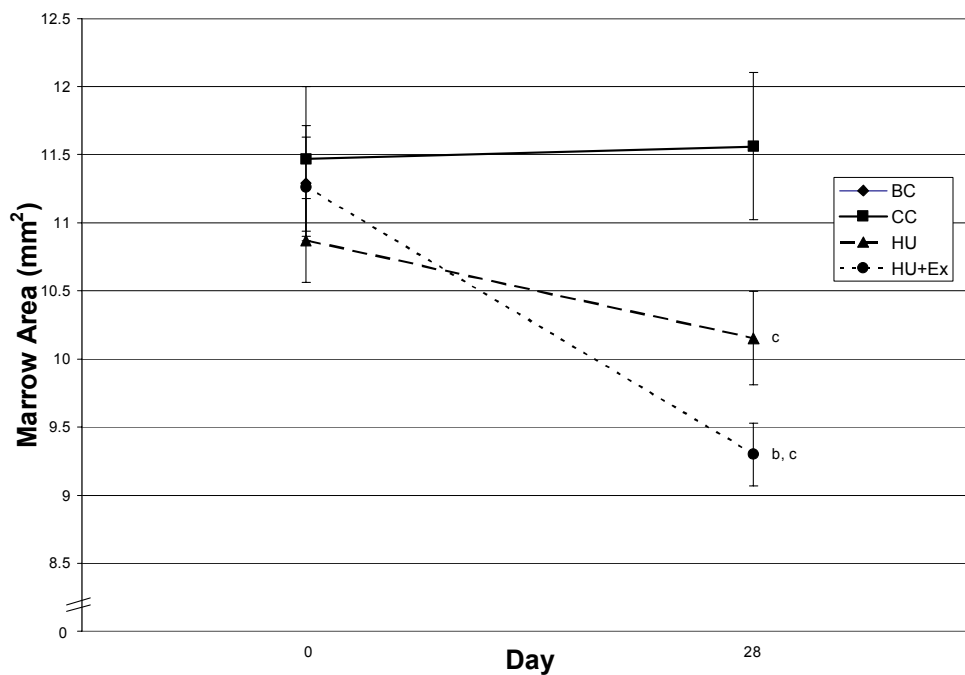


Figure 21: Marrow area of the tibial metaphysis during 28 days of unloading. The left leg of HU+Ex received muscle contraction exercise. *b*:  $P<0.05$  vs. day 0 within group; *c*:  $P<0.05$  vs. CC values.

#### 4.4.3 Cortical area

The metaphyseal cortical area (Figure 22) for the HU group was significantly lower than both HU+Ex and CC after 28 days (9.6% and 9.8%, respectively;  $P < 0.001$ ). There were no significant differences among groups at day 0. The countermeasure maintained cortical areas near control levels during disuse. Post hoc comparisons showed that there were no significant changes within groups with respect to time ( $P > 0.05$ ).

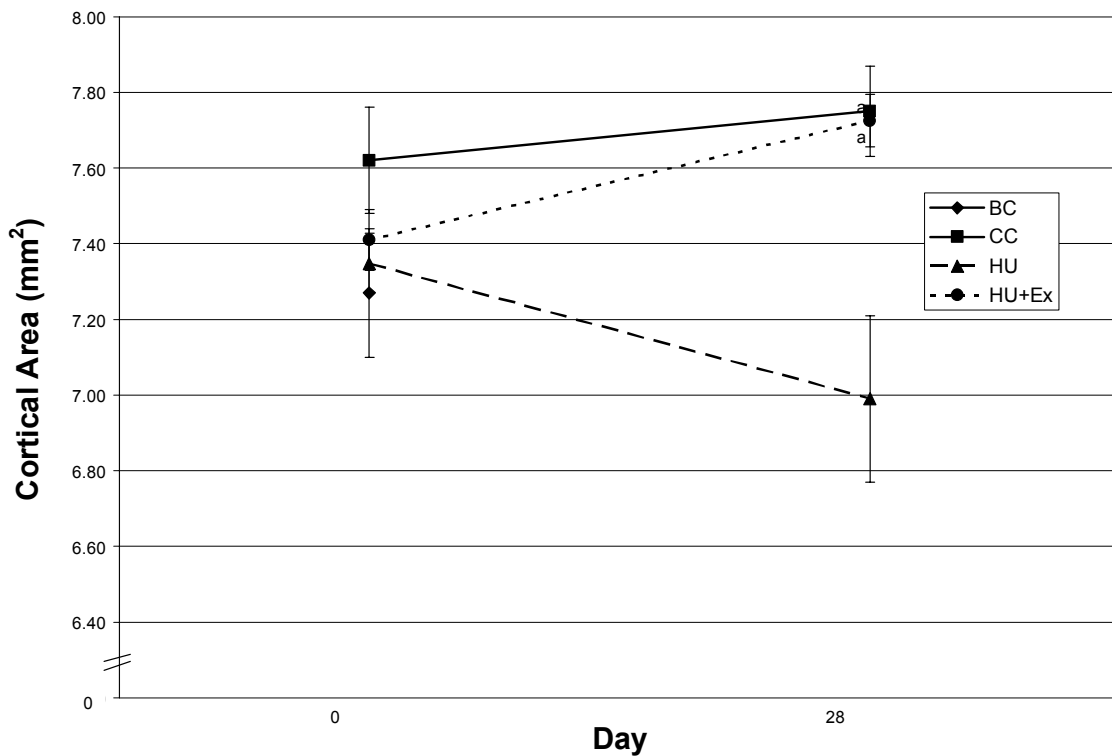


Figure 22: Cortical area of the tibial metaphysis during 28 days of unloading. The left leg of HU+Ex received muscle contraction exercise. *a*:  $P < 0.05$  vs. HU values.

## 4.5 Tibial metaphysis volumetric bone mineral density (vBMD)

### 4.5.1 Total vBMD

Results for the total vBMD at the tibial metaphysis are summarized graphically in Figure 23. After 28 days, the HU+Ex group had vBMD values 16.8% higher than HU ( $680.72 \pm 21.29$  mg/cm<sup>3</sup> vs.  $582.86 \pm 32.49$  mg/cm<sup>3</sup>,  $P = 0.017$ ). Previous results showed

that the HU+Ex vBMD levels are 11% greater than those of HU values<sup>19</sup>. HU+Ex values were also 13.4% larger than vBMD values for CC at day 28 ( $680.72 \pm 21.29 \text{ mg/cm}^3$  vs.  $600.33 \pm 32.20 \text{ mg/cm}^3$ ,  $P=0.025$ ). For both CC and HU, there was no statistical difference in vBMD levels over the 28 day period ( $P=0.474$  and  $P=0.141$ , respectively). The countermeasure increased vBMD levels from day 0 to day 28, showing a 14.2% rise for HU+Ex ( $680.72 \pm 21.29 \text{ mg/cm}^3$  vs.  $596.19 \pm 25.46 \text{ mg/cm}^3$ ,  $P<0.001$ ).

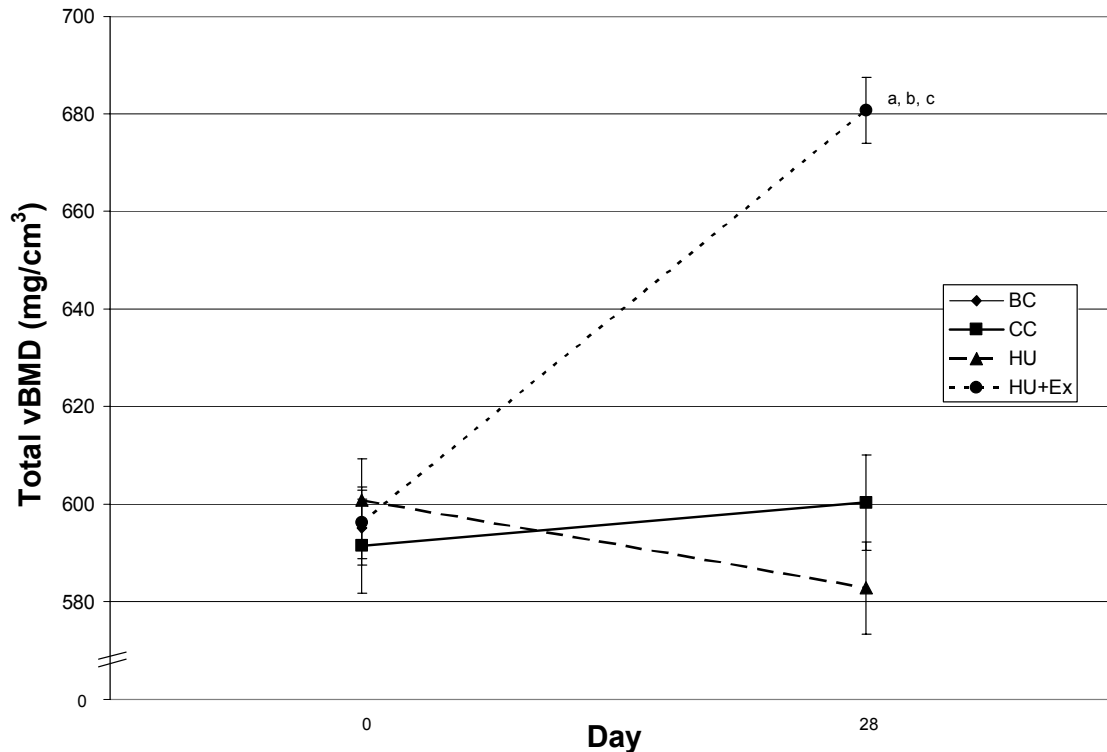


Figure 23: Total vBMD of the tibial metaphysis during 28 days of unloading. The left leg of HU+Ex received muscle contraction exercise. *a*:  $P<0.05$  vs. HU values; *b*:  $P<0.05$  vs. day 0 within group; *c*:  $P<0.05$  vs. CC values.

A two-way ANOVA was performed to determine statistical significance among groups over time. Mean values of the groups at day 0 were not statistically different, indicating that all the groups started at the same vBMD. This confirms that the block assignment of rats by body weight and total vBMD at day 0 was successful in producing virtually identical mean total vBMD values at day 0. The mean values were significantly different at day 28 ( $P=0.0008$ ). Post hoc comparisons showed that total vBMD for CC and HU were not significantly different ( $P=0.161$ ), but the HU+Ex mean value was much

higher than those for both CC and HU ( $P < 0.001$ ). The exercise training during disuse prevented losses of total vBMD at the proximal tibia.

#### 4.5.2 Cancellous vBMD

The cancellous vBMD in the proximal tibia (Figure 24) for HU+Ex was found to be not statistically different from either that for CC or HU at day 28 ( $P = 0.080$ ; see Table 1, p.62, for values). While HU values were 15% lower than HU+Ex after 28 days ( $224.18 \pm 30.05 \text{ mg/cm}^3$  vs.  $263.75 \pm 37.41 \text{ mg/cm}^3$ ), the difference is not significant ( $P = 0.060$ ). HU vBMD levels were 11.4% lower than CC values, but this difference was not statistically significant. Mean values among groups were not significantly different at day 0, or at day 28. The change in vBMD with respect to time was not significant for any of the groups ( $P = 0.199$ ).

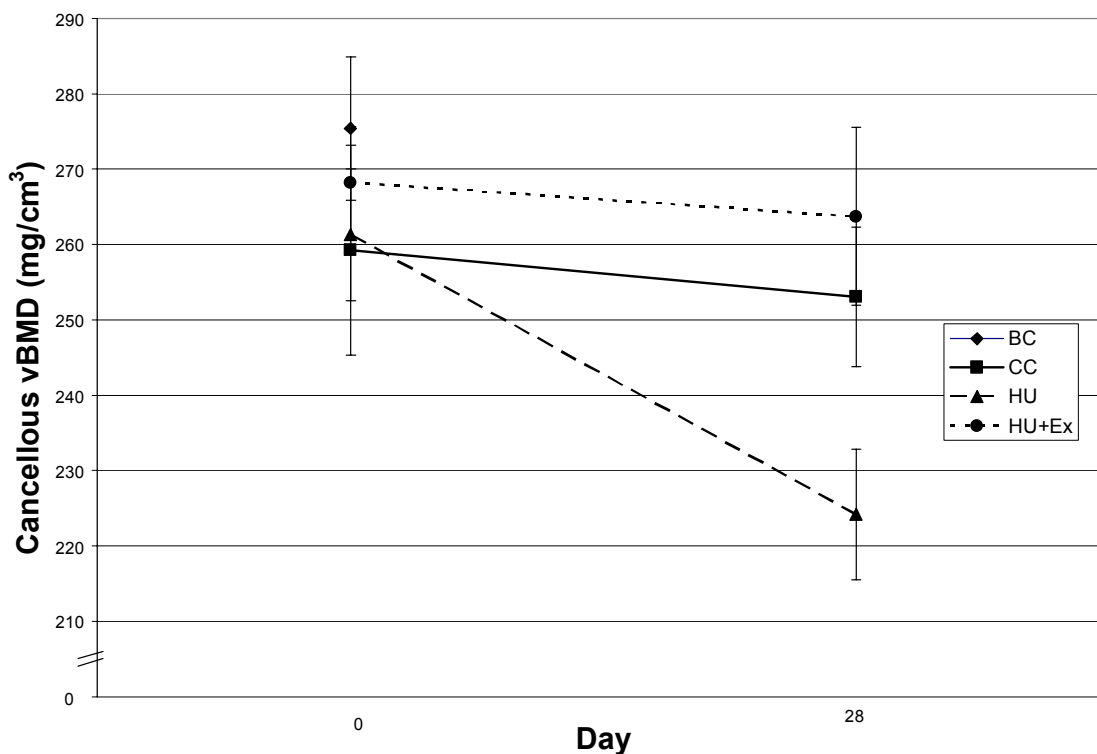


Figure 24: Cancellous vBMD of the tibial metaphysis during 28 days of unloading. The left leg of HU+Ex received muscle contraction exercise. There was no statistical significance observed for comparisons among groups or over time within groups.

#### 4.5.3 Cortical vBMD

After 28 days of the countermeasure treatment, the HU+Ex group had 6.9% greater cortical vBMD values than did both HU and CC rats ( $1141.43 \pm 27.96 \text{ mg/cm}^3$  vs.  $1067.92 \pm 45.78 \text{ mg/cm}^3$ ,  $P < 0.001$ ;  $1141.43 \pm 27.96 \text{ mg/cm}^3$  vs.  $1067.45 \pm 28.86 \text{ mg/cm}^3$ ,  $P < 0.001$ ) (Figure 25). The countermeasure was successful in not only maintaining vBMD levels, but also effectively increased the vBMD above that of the control group. The HU+Ex group increased 8.9% over the course of the study ( $P < 0.001$ ). The cortical vBMD for HU and CC groups did not change significantly with time over the duration of the study.

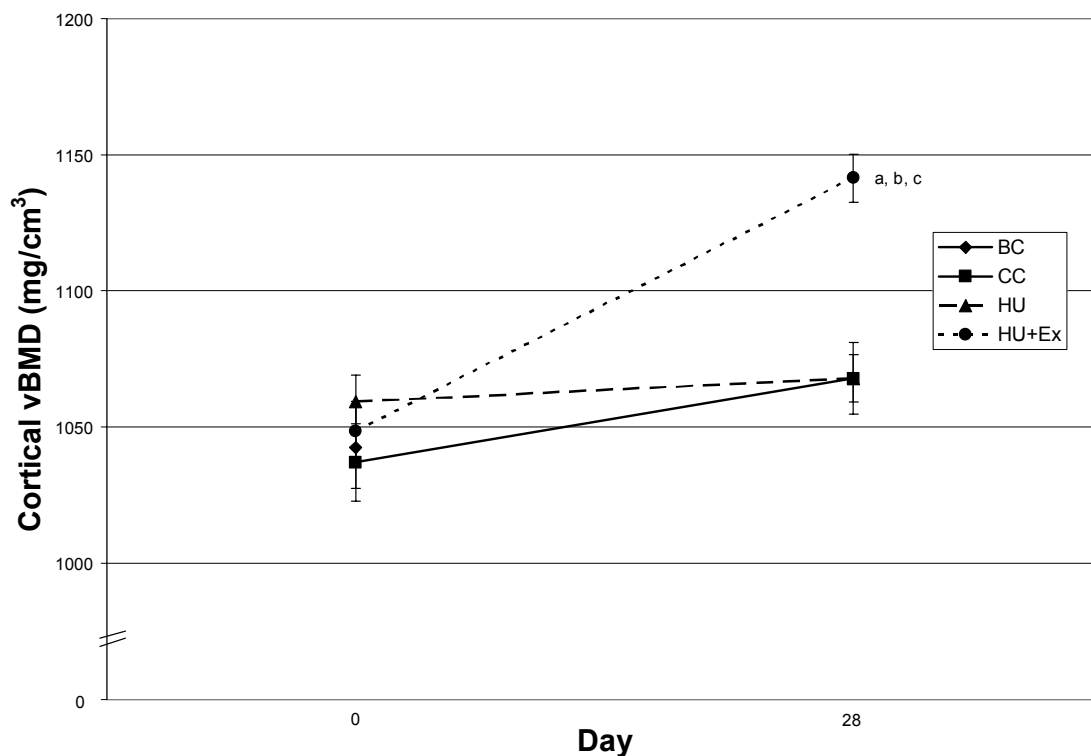


Figure 25: Cortical vBMD of the tibial metaphysis during 28 days of unloading. The left leg of HU+Ex received muscle contraction exercise. *a*:  $P < 0.05$  vs. HU values; *b*:  $P < 0.05$  vs. day 0 within group; *c*:  $P < 0.05$  vs. CC values.

#### 4.6 Midshaft tibial results

All results from pQCT analyses at the midshaft of the tibia are summarized in Table 2, (p.63). The following sections contain graphical presentations of the results, along with brief explanations of the statistical comparisons and results.

#### 4.6.1 Midshaft total BMC

The countermeasure exerted an effect on the total BMC of the tibial midshaft (Figure 26). The HU+Ex group exhibited significantly higher BMC values at day 28 than did HU rats, with a difference of 14.2% ( $8.29 \pm 0.57$  mg vs.  $7.26 \pm 0.46$  mg,  $P < 0.001$ ). In addition, HU+Ex values were 7.8% larger than CC ( $8.29 \pm 0.57$  mg vs.  $7.69 \pm 0.45$  mg,  $P = 0.016$ ). There were no significant differences among groups at day 0.

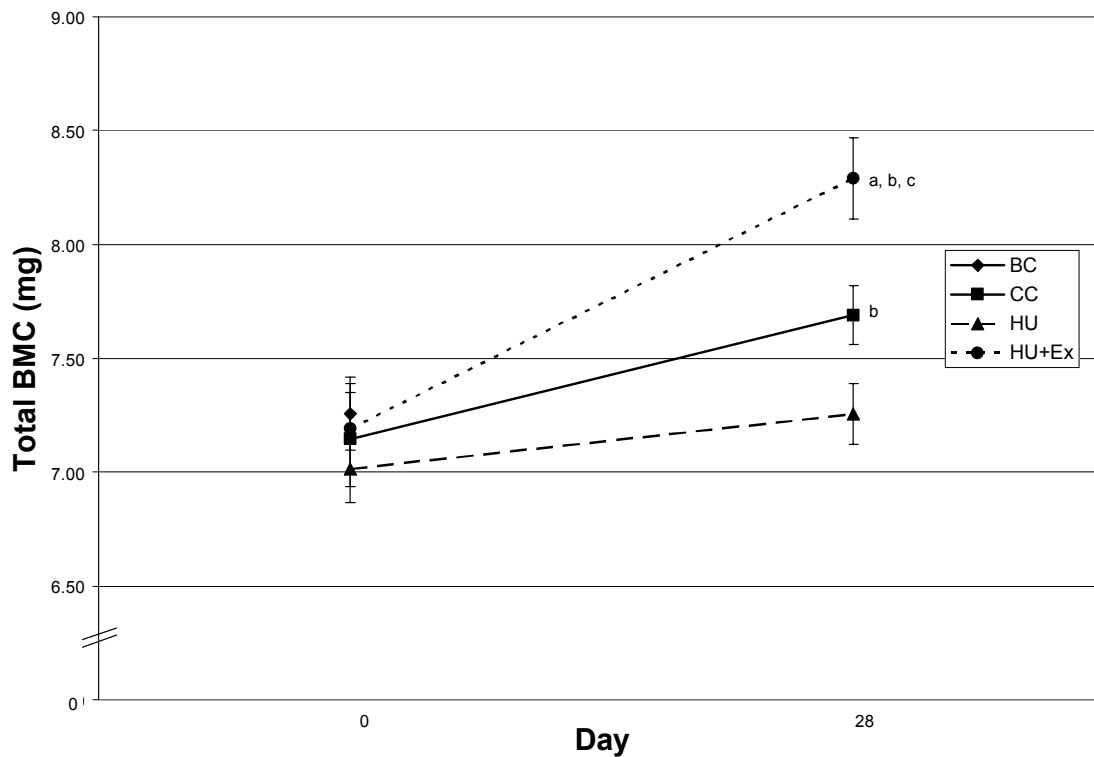


Figure 26: Total BMC of the tibial midshaft during 28 days of unloading. The left leg of HU+Ex received muscle contraction exercise. *a*:  $P < 0.05$  vs. HU values; *b*:  $P < 0.05$  vs. day 0 within group; *c*:  $P < 0.05$  vs. CC values.

Post hoc comparisons showed a significant effect due to time for the HU+Ex and CC groups. The countermeasure increased the BMC values over 28 days by 15.3% ( $P < 0.001$ ). The CC group also increased by 7.7% ( $P = 0.009$ ). There was no significant change in the HU group over the course of the study.

#### 4.6.2 Midshaft cortical BMC

A two-way ANOVA analysis showed significant changes in the cortical BMC of the tibial midshaft (Figure 27). The cortical BMC levels of the HU+Ex group after 28 days were significantly greater than both the HU values (13.6%,  $P<0.001$ ) and the CC values (7.7%,  $P=0.010$ ). There was no significant difference among groups at day 0.

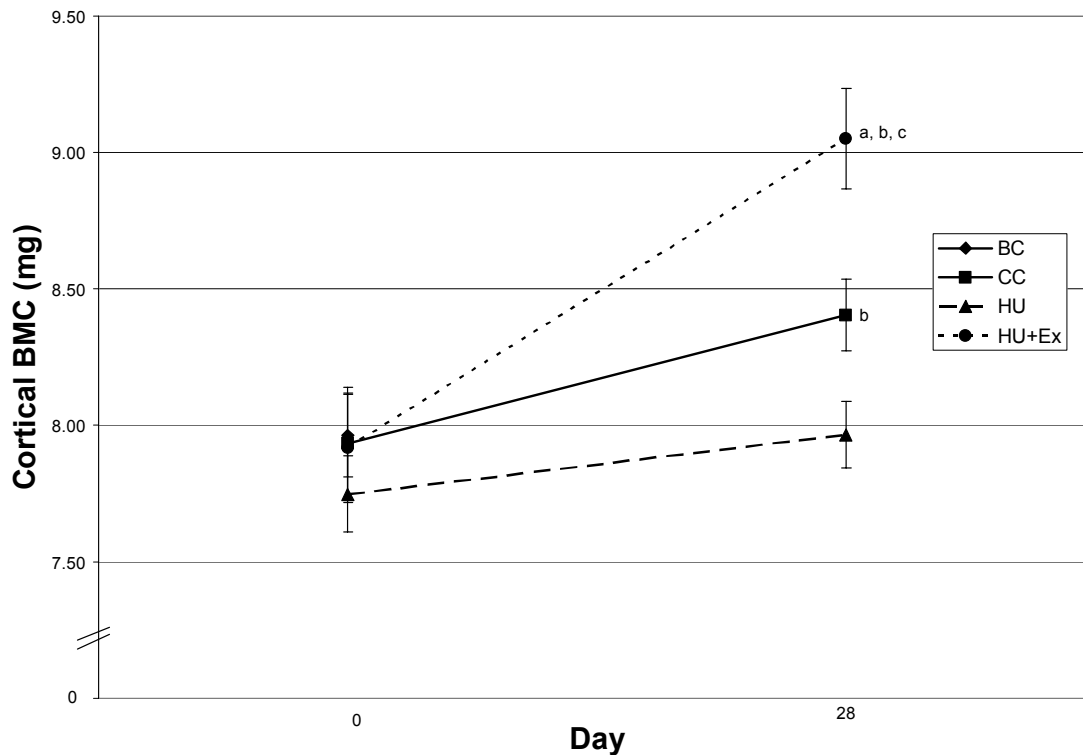


Figure 27: Cortical BMC of the tibial midshaft during 28 days of unloading. The left leg of HU+Ex received muscle contraction exercise. *a*:  $P<0.05$  vs. HU values; *b*:  $P<0.05$  vs. day 0 within group; *c*:  $P<0.05$  vs. CC values.

Post hoc pairwise comparisons showed a 14.3% increase in BMC levels for HU+Ex over 28 days ( $9.05 \pm 0.58$  mg vs.  $7.92 \pm 0.70$  mg,  $P<0.001$ ). The CC group also increased over 28 days, with an increase of 5.9% ( $8.40 \pm 0.46$  mg vs.  $7.93 \pm 0.72$  mg,  $P=0.022$ ). The countermeasure maintained and raised BMC levels above that of the control group after 28 days of disuse.

#### 4.6.3 Midshaft total area

A two-way ANOVA analysis of the midshaft total area (Figure 28) did not reveal any significant differences among groups at day 0 or 28 ( $P=0.126$ ). Post hoc pairwise comparisons showed a significant increase over 28 days in total area for the HU+Ex group and the CC group. The HU+Ex values increased 9% ( $P<0.001$ ), and the CC group total area increased of 7% ( $P<0.001$ ). The countermeasure maintained periosteal apposition. The total area of the HU group did not significantly change over time.

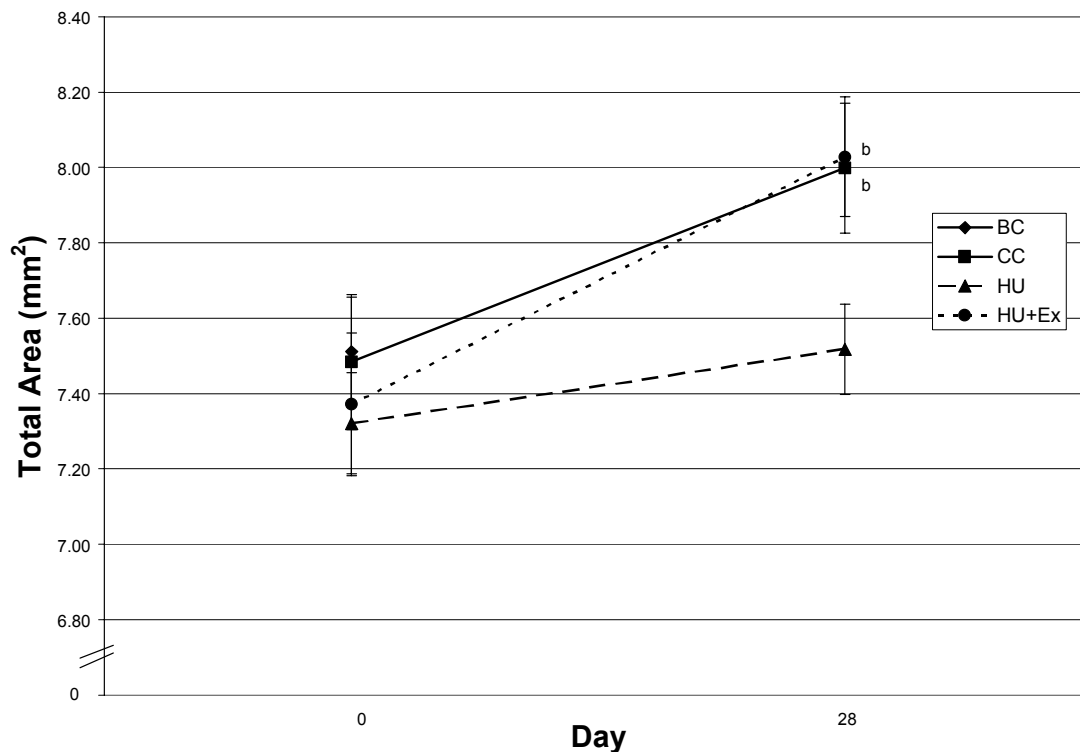


Figure 28: Total area of the tibial midshaft during 28 days of unloading. The left leg of HU+Ex received muscle contraction exercise. *b*:  $P<0.05$  vs. day 0 within group.

#### 4.6.4 Midshaft cortical area

Analysis of the cross-sectional cortical area data (Figure 29) of the HU+Ex group showed 13.2% greater areas than the HU group ( $P<0.001$ ) and 6.6% larger areas than the CC group ( $P=0.022$ ). The HU group cortical area was 5.8% smaller than CC values ( $P=0.035$ ). The mean values of the treatment groups were not significantly different at day 0.

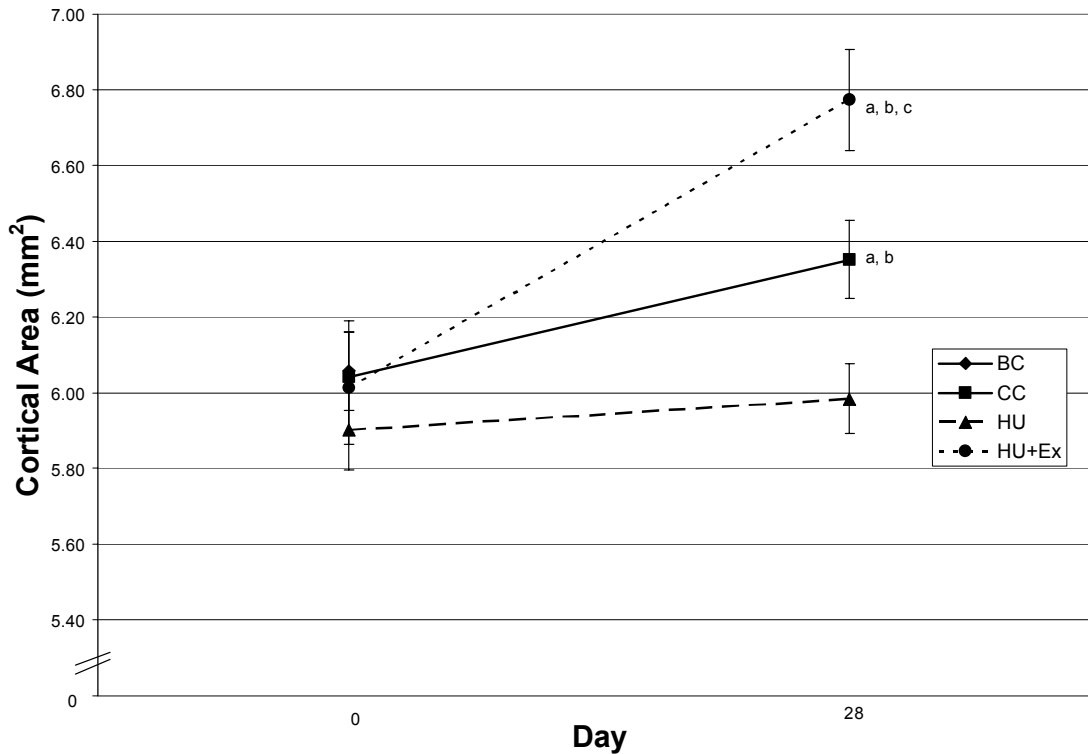


Figure 29: Cortical area of the tibial midshaft during 28 days of unloading. The left leg of HU+Ex received muscle contraction exercise. *a*:  $P < 0.05$  vs. HU values; *b*:  $P < 0.05$  vs. day 0 within group; *c*:  $P < 0.05$  vs. CC values.

Post hoc comparisons showed statistical increases in the cortical area over time for the HU+Ex group (+12.7%,  $P < 0.001$ ) and the CC group (+5.1%,  $P = 0.040$ ). The HU group's cortical area did not change significantly during the course of the study. The countermeasure stimulated a gain the cortical area above that of the control group.

#### 4.6.5 Midshaft marrow area

The marrow area of the tibial midshaft (Figure 30) was not significantly different among groups at day 0 or at 28 ( $P = 0.381$ ). The marrow area of the groups did not change significantly over time ( $P = 0.294$ ). Because the data were not normally distributed and the equal variance test failed, a post-hoc comparison was not available for the statistical analysis.

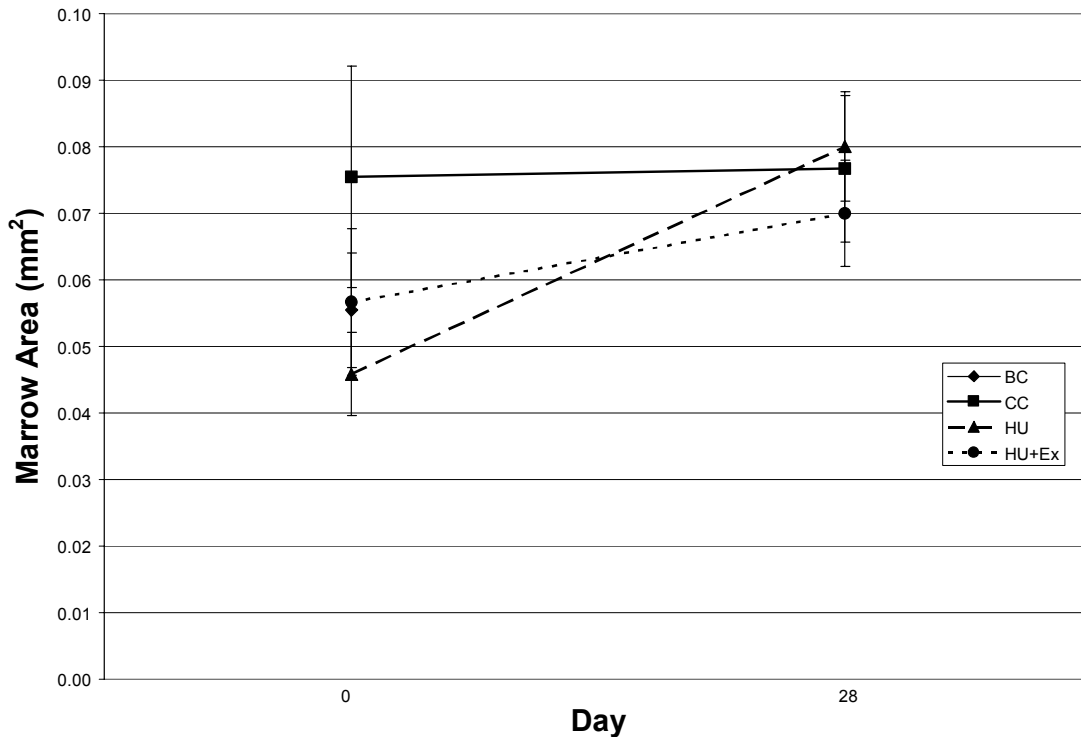


Figure 30: Marrow area of the tibial midshaft during 28 days of unloading. The left leg of HU+Ex received muscle contraction exercise. There were no statistically significant differences observed among groups or over time.

#### 4.6.6 Midshaft total vBMD

Total vBMD values at the tibial midshaft (Figure 31) were significantly greater in the HU+Ex group as compared to those in the HU and CC groups. HU+Ex mean vBMD levels were 7% greater than HU ( $1032.51 \pm 27.21 \text{ mg/cm}^3$  vs.  $965.33 \pm 35.03 \text{ mg/cm}^3$ ,  $P < 0.001$ ), and 7.2% higher than CC values ( $1032.51 \pm 27.21 \text{ mg/cm}^3$  vs.  $963.50 \pm 42.30 \text{ mg/cm}^3$ ,  $P < 0.001$ ). Post hoc comparisons showed statistical increases in vBMD levels (5.9%) for the HU+Ex group over 28 days ( $1032.51 \pm 27.21 \text{ mg/cm}^3$  vs.  $975.47 \pm 23.90 \text{ mg/cm}^3$ ,  $P < 0.001$ ). The countermeasure was effective in raising vBMD levels during disuse not only above those of the HU group, but also above the control group, and in showing a significant increase over time.

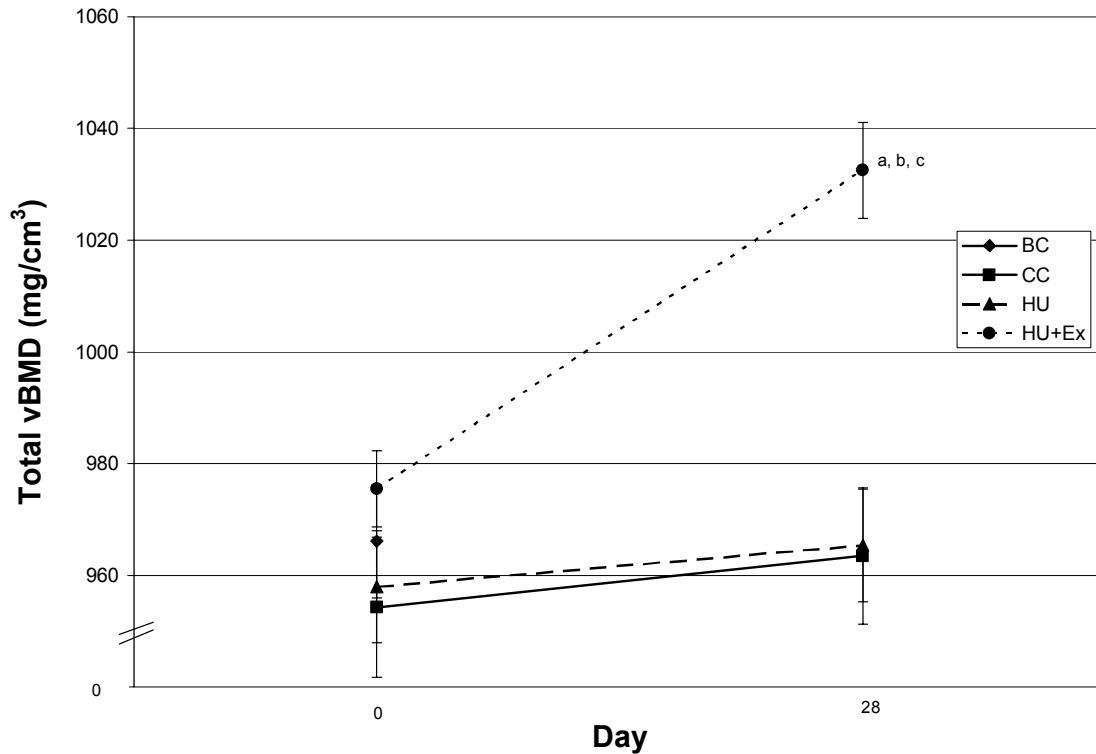


Figure 31: Total vBMD of the tibial midshaft during 28 days of unloading. The left leg of HU+Ex received muscle contraction exercise. *a*:  $P < 0.05$  vs. HU values; *b*:  $P < 0.05$  vs. day 0 within group; *c*:  $P < 0.05$  vs. CC values.

#### 4.6.7 Midshaft cortical vBMD

Results for total vBMD at the midshaft of the tibia are summarized graphically in Figure 32. A two-way ANOVA analysis showed that after 28 days, there was no significant difference among groups in cortical vBMD of the tibial midshaft ( $P = 0.694$ ). Post hoc pairwise comparisons did not reveal any statistically significant changes in each group over the 28 day period.

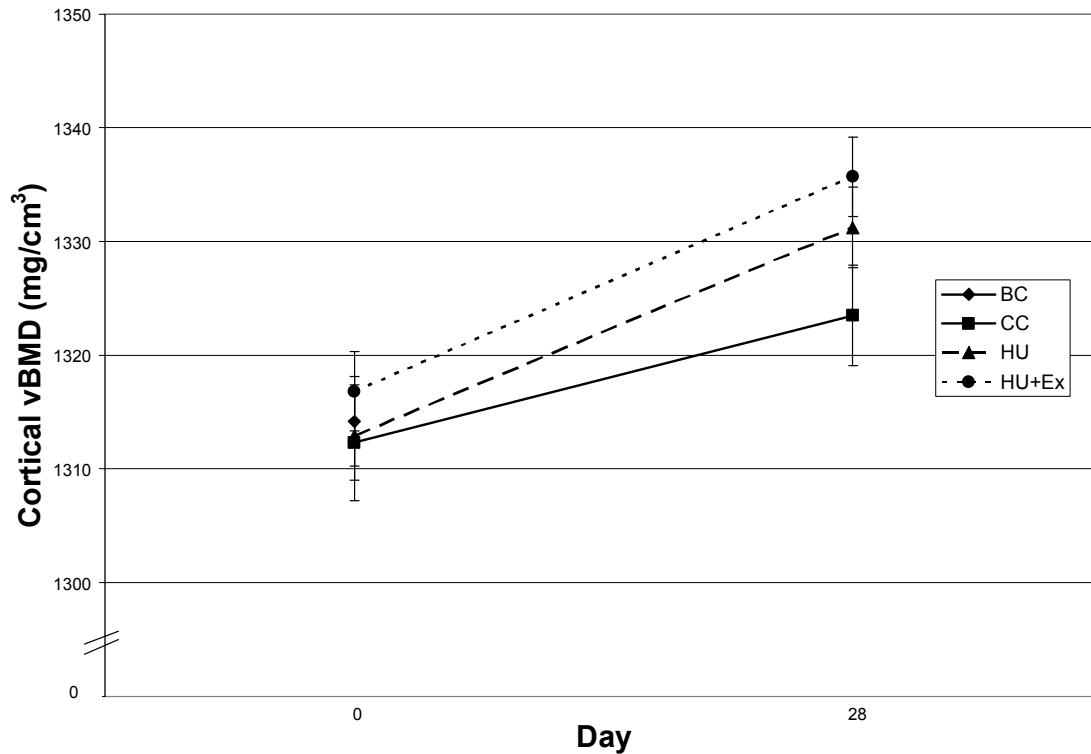


Figure 32: Midshaft cortical vBMD after 28 days of unloading. The left leg of HU+Ex received muscle contraction exercise. There were no statistically significant differences observed among groups or over time.

#### 4.6.8 Midshaft cortical shell thickness

The thickness of the cortical shell at the tibial midshaft (Figure 33) was significantly larger for the HU+Ex group than both the HU group and the CC group. The countermeasure induced thicknesses 14.1% greater than the HU group ( $0.97 \pm 0.04$  mm vs.  $0.85 \pm 0.04$  mm,  $P < 0.001$ ) and 10.2% larger than CC values ( $0.97 \pm 0.04$  mm vs.  $0.88 \pm 0.05$  mm,  $P < 0.001$ ). The HU group and CC group were not statistically significant from one another. There was no difference among groups at day 0. Pairwise comparisons revealed a significant increase in thickness for the HU+Ex group over 28 days (11.5%,  $P < 0.001$ ).

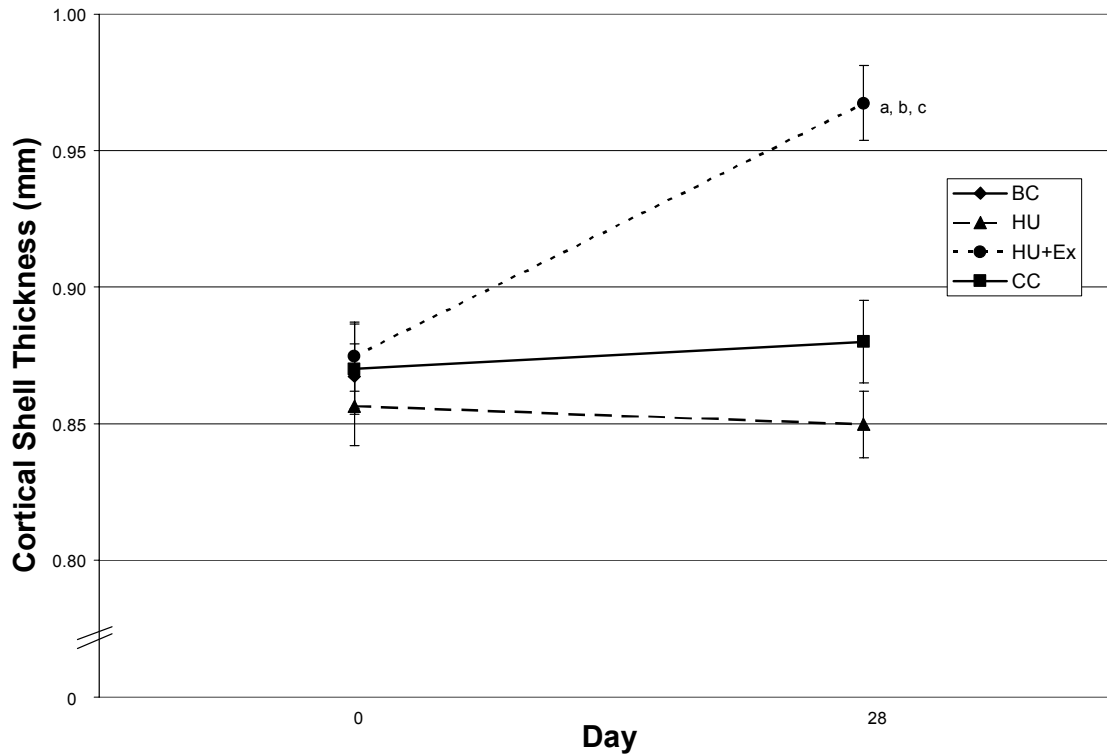


Figure 33: Cortical shell thickness of the tibial midshaft during 28 days of unloading. The left leg of HU+Ex received muscle contraction exercise. *a*:  $P < 0.05$  vs. HU values; *b*:  $P < 0.05$  vs. day 0 within group; *c*:  $P < 0.05$  vs. CC values.

#### 4.7. Mechanical properties

RPC testing was used to determine differences in the intrinsic mechanical properties of the tibial metaphysis. All results for mechanical properties from RPC testing are summarized in Table 3 (p.63). The countermeasure was effective in improving the mechanical integrity after 28 days of disuse. The ultimate stress (Figure 34) of the HU+Ex group was found to be 268% greater than the HU mean values ( $2.28 \pm 1.48$  MPa vs.  $0.62 \pm 0.53$  MPa,  $P < 0.05$ ), and 175% greater than CC ( $2.28 \pm 1.48$  MPa vs.  $0.83 \pm 0.59$  MPa,  $P < 0.05$ ). The HU group's ultimate stress was not significantly lower than that of CC rats.

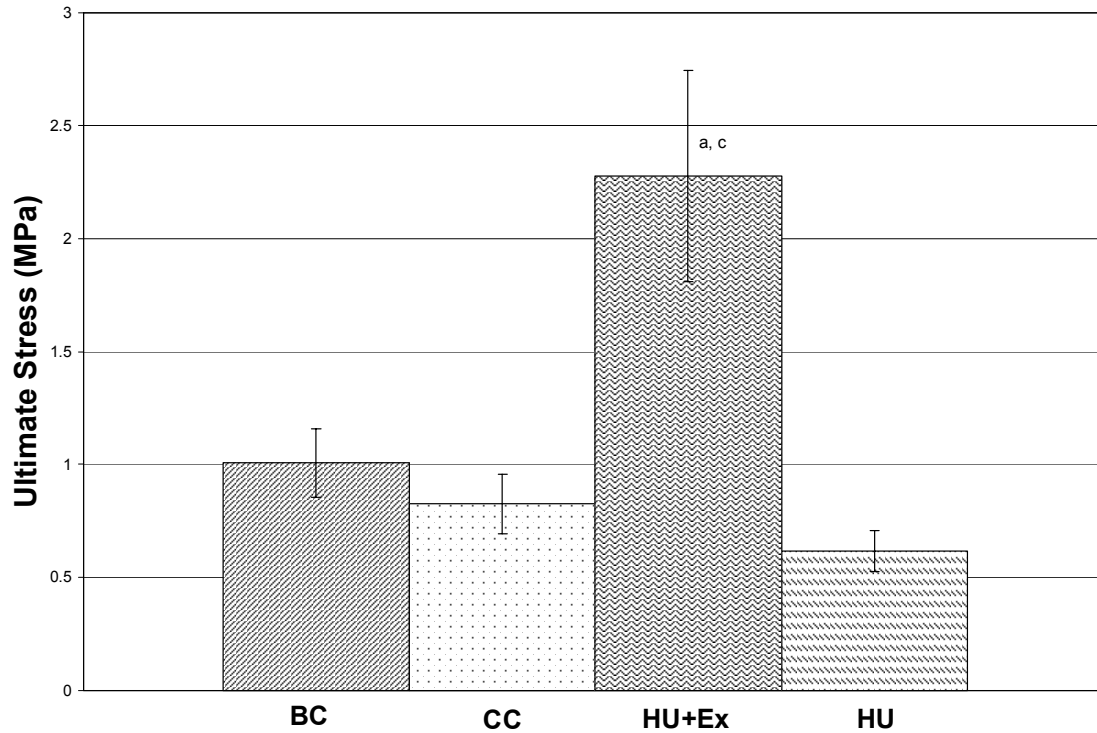


Figure 34: Ultimate stress of the tibial metaphysis after 28 days of unloading. The left leg of HU+Ex received muscle contraction exercise. *a*:  $P < 0.05$  vs. HU values; *c*:  $P < 0.05$  vs. CC values.

The elastic modulus was not found to be significantly impacted by the countermeasure (Figure 35). None of the group's values were statistically different from each other ( $P = 0.896$ ), although the HU+Ex modulus was 26.4% higher than that of HU, and 14.8% lower than that of CC.

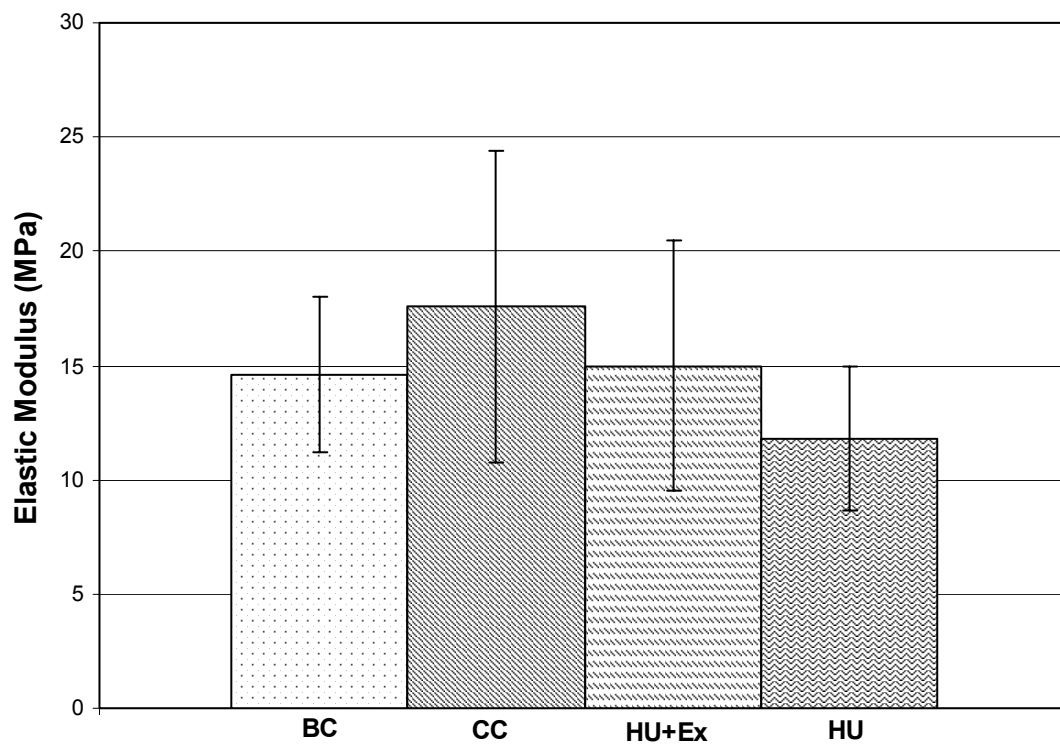


Figure 35: Elastic modulus of the tibial metaphysis after 28 days of unloading. The left leg of HU+Ex received muscle contraction exercise. There was no statistical significance between groups.

## 5. DISCUSSION

### 5.1. Purpose and general findings

The aim of the study was to evaluate the effects of a resistive exercise training regimen as a countermeasure to bone loss induced by hindlimb suspension. The tibial metaphysis exhibits decreases in bone mechanical properties, mineral content, and density in a disuse environment. The exercise protocol utilized in this study maintained bone mineral content and density levels at the level of weight-bearing control animals and in some cases exceeded those of controls at the tibial metaphysis. Values for total BMC and total vBMD at the tibial metaphysis were higher in the exercise group than the unexercised group. In addition to changes at the tibial metaphysis, total BMC and vBMD at the tibial midshaft were significantly higher for the exercised limb. For many measured parameters, the exercise group values were elevated above those of both the cage control and the non-exercised HU group.

At the tibial metaphysis, there was a small gain in total BMC as a result of the exercise training, but the gain was not different from that observed in the CC group. As the total vBMD is the total BMC normalized for the volume of the scan slice, this indicates that the gain in vBMD due to exercise resulted from the decreased area rather than an increase in density.

Because bone can form on both the outer (periosteal) and inner (endocortical) surfaces of the bone, it is important to look at the changes in bone cross-sectional area to determine where new bone was added. The total area at the proximal tibia decreased with disuse (both HU and HU+Ex). The marrow area also decreased with disuse, but cortical area did not change. Based on these observations, one can conclude that the gain in bone occurred on the endosteal surface (the surface of the marrow cavity). This also indicates that the gain was largely in the cortical compartment. At the tibial midshaft, the total area increased as a result of the exercise regimen; the cortical area also increased. However, there was no significant change in marrow area, so bone appears to have formed on the periosteal surface.

The total vBMD at the proximal tibia for the HU+Ex group was significantly higher than values for both the CC and HU groups after 28 days and increased

significantly over the 28-day period. The total vBMD includes both cancellous vBMD and cortical vBMD at the metaphysis. In order to evaluate which bone compartment contributed the most to the total vBMD, one must evaluate each of the compartments separately in light of total gain. Because the cancellous vBMD did not exhibit significant changes for any of the groups, it can be concluded that the increase in vBMD due to exercise is largely a result of the increase in cortical bone.

The presence of an HU group to represent the disuse model was included to account for any systemic effects caused by the exercise regimen on the unexercised right leg of the HU+Ex group. However, as noted in the statistics section (p. 23), there was no statistical difference in mechanical properties between the HU group and the right leg of the HU+Ex group. While the extra HU group is beneficial for producing a more robust data set, it is not necessary as a disuse model, and the contralateral right limb of the exercise group can continue to serve as the disuse model.

## **5.2 Procedural caveats**

### *5.2.1 Hindlimb suspension*

Hindlimb suspension provides a ground-based model for the simulation of microgravity effects from space flight. Skeletal adaptations to disuse are similar to those observed in rats during spaceflight based on histomorphometric analyses of bone cell activity<sup>23</sup>. However, the difference in bone response may vary between hindlimb suspension and space flight. Inconsistencies in osteoclastic activity between suspended rats and rats in space flight suggest that bone loss in each microgravity situation occurs differently<sup>24</sup>. Osteoid surfaces in cancellous regions were lost in both conditions but in larger amounts for space flight (55% less osteoid surfaces vs. 22% lower osteoid surfaces for hindlimb suspension). Bone formation decreases in space flight, but in hindlimb suspended configurations, the bone formation is reduced only slightly while resorption is increased. The HU model is not completely analogous to actual space flight, but the bone exhibits similar behavior in each condition, thus HU has become a widely accepted and useful animal model.

The hindlimb suspension model creates issues related to animal welfare. The sling by which the animal is suspended is glued onto the animal's skin. This could cause problems with loss of blood flow to the tail, causing sores on the tail. If not corrected, this results in a necrotic tail, and the animal must be immediately sacrificed for humane reasons. This occurs less than 5% of the time in the researcher's laboratory.

In addition to impeding blood flow, the sling also has the ability to slide off the tail. It is attached with marine glue, and as skin cells come loose, the sling can come off, allowing the animal to ambulate on all four limbs. This creates unwanted loading and removes the true disuse environment. If this occurs frequently, the model becomes inadequate for simulating microgravity.

### *5.2.2 Simulated resistive training via electrical muscle stimulation*

During electrical muscle stimulation, the foot is attached to the servo motor foot pedal by a plastic foot mold and tape. While the forefoot is securely taped to the pedal, the heel is able to come off of the pedal. It cannot be taped down because this would hinder ankle movement during rotation of the foot pedal. It is desirable for the heel to maintain consistent contact in order to transmit the full force of the contraction to the foot plate, but this may not be achieved in all cases.

The knee is clamped at a 90 degree angle between the axes of the femur and the tibia. Several times during training sessions, the force of the contractions was stronger than the clamp, allowing the knee to move during the exercise. In such occurrences, the operator would adjust and supplement the clamp to ensure its correct positioning.

Stimulated muscle contractions are not equivalent to voluntary exercise, largely because the animal is anesthetized during the exercise training. The sympathetic nervous system under anesthesia affects blood flow to the skeletal muscles and internal organs. In a rat model, the animal under anesthesia during stimulated exercise exhibits lower sympathetic nervous system (SNS) activation in the skeletal muscles than in the kidneys<sup>25</sup>. This lower SNS activity results in increased vasoconstriction in the skeletal muscles. Thus during anesthetized exercise, there is less blood flow to the muscles than to internal organs, making this type of exercise less physiological than voluntary exercise.

In addition, fewer motor units are activated under anesthesia than during voluntary contractions of the same intensity. This causes a different muscle recruitment pattern.

However, the stimulated muscle exercise has some advantages that true physiological exercise does not. It allows for the control of the velocity of movement, the angle of rotation, and the level of exercise intensity (at least to some degree). Typical voluntary exercises in animal models do not have methods of consistently and quantitatively controlling all of these variables. The direct control of torque, movement, and angle makes this mode of exercise beneficial and unique in studying the effects of exercise.

### *5.2.3 Changes in material properties*

The ultimate stress of the HU+Ex group bones was significantly higher than both the CC and HU groups (Figure 34, p.43). The stimulated resistance training raised the ultimate stress level high above that of normal weight-bearing rats. The CC group, however, did not exhibit significant differences in ultimate stress as compared to that of the HU group, but there was a trend for lower HU values compared to CC rats (mean HU ultimate stress was 25% lower than CC). The intensity of the resistance training not only kept stress levels from being lower as a result of disuse, but it also elevated the ultimate stress much higher than the control group.

The elastic modulus was not significantly different among any of the groups (Figure 35, p.44). These results were not what were expected based on previous similar studies measuring mechanical properties<sup>19</sup>. The subjectivity of interpreting the data from the force-displacement plots created by the RPC testing is an issue that has yet to be resolved. In order to determine such intrinsic properties as the ultimate strength and elastic modulus, the extrinsic values such as maximum force and stiffness must first be determined from the mechanical testing data. The operator manually inspects the plots and fits a regression line to the linear portion of the plot, and the slope of this line defines the stiffness. The maximum force is straightforward in definition and concept, but in many cases, the scatter and variation in load data introduce substantial interpretation and objective judgment in determining the maximum force value. Similar subjectivity is also involved in determining the stiffness. In this case, one must take into account any

“preload” that is present on the tested sample. The preload is a minimal amount of loading (as close to zero as possible) applied by lowering the Instron crosshead onto the sample, and is used to hold the sample in place before the test is started without actually applying significant load. In some cases, the applied preload was much larger than zero, thus increasing the y-intercept of the plot and decreasing the slope and thereby substantially reducing the number of data points available for determining the linear region. This may have introduced more variability than is customary in the values for stiffness, and correspondingly in the elastic modulus, which may have contributed to the lack of significant differences.

#### *5.2.4 Anesthesia control and weight loss*

The results of the body weights after 28 days indicated a drop in weight for the HU+Ex group, while the HU group did not change. The reason for this lack of change could be due to the fact that the HU group did not receive anesthesia during the 28 day period. However, each animal in the HU+Ex group was anesthetized for 30-40 minutes every other day for 28 days. This likely caused the reduction in weight. In future studies, an anesthesia control would be beneficial to verify that the weight loss is not due to the exercise treatment alone.

The reduction of weight in the HU+Ex group is a strong argument for the effectiveness of the exercise treatment in mitigating bone loss. Because the vBMD went up while the weight went down, it can be concluded that there was indeed an increase in bone density as a result of the exercise. Also, the HU group did not lose or gain weight, so the bone loss seen in that group cannot be attributed to overall weight loss.

### **5.3 Comparison with previous HU+Exercise studies with rodents**

This section will discuss different exercise interventions for rat disuse models. It will address issues such as whether the loading paradigm is physiological, if the loads applied are physiological in magnitude, and what material properties are evaluated in the study.

### 5.3.1 *Electric muscle stimulation of the free-hanging limb during HU*

Forty-five male Wistar rats (9 weeks old) received muscle stimulation of the left leg for 10 days<sup>26</sup>. The animals were divided into five groups: CC, HU, HU+ stimulation at 1Hz, HU+ stimulation at 50Hz, and HU+ stimulation at 100Hz. The exercise protocol for the 50Hz stimulations consisted of stimulation lasting for 2s, with 3s rest between contractions, for four hours. This was repeated after 6 hours of recovery, for a total of 8 hours of exercise per day. The animals exercised twice a day for 10 days, and were sacrificed 12 hours after the last exercise session.

There were no differences in the tibial or femoral vBMD (measured by dual energy x-ray absorptiometry, or DEXA) among any of the exercise-stimulated groups and the HU control. However, for both the femoral and tibial BMC, the 50Hz group was significantly greater than HU after 10 days of exercise. In addition, the BMC of the tibia (50Hz exercise group) was greater than that of its unexercised right leg. These changes in BMC contribute evidence to support the theory that muscle-stimulated exercise minimizes the detrimental effects of disuse due to hindlimb unloading and corroborates the results in the current study that demonstrated increases in BMC with exercise.

This study did not consider the effect on mechanical properties related to HU and exercise, nor did it quantify the magnitude of loading induced on the tibia by the muscle contractions. The investigators applied a rigorous muscle stimulation exercise regimen in terms of number of loading cycles, but did not measure the loads. Since the legs were not restrained in any way during muscle stimulation, the loads on the bone were likely quite low. It has been previously noted that the magnitude of loading affects the osteogenic response of the bone<sup>27</sup>. The lack of response in BMD may be due to the questionable loading. Another possible factor could be the short duration of the study (only 10 days). The resorptive phase in cancellous bone lasts for approximately 10 days, while the bone formation phase can take up to three months<sup>4</sup>. In order to observe the results of the full cycle, the study should have a duration long enough to observe the effects of bone formation from countermeasures. Also, the rest period between contractions was not long enough to allow recovery, thus making the exercise one long session instead of many shorter sessions. Previous studies have shown that the osteogenic response is greater when loading is broken up into several bouts rather than one long bout<sup>38</sup>.

### 5.3.2 *Voluntary flywheel exercise of HU rats*

Fourteen male Sprague-Dawley rats (six months old) were employed in this study<sup>28</sup>. All animals were conditioned to perform a leg extension while standing in a vertical box to depress a lever in response to light stimulus, which mimics leg squats as performed by humans. Once conditioned, the rats were divided into control, hindlimb suspended (HS), or HS with resistive exercise training (HSRT). The HSRT rats then performed the squat-like exercise in a horizontal box using a flywheel to create resistance while maintaining hindlimb suspension. The rats perform two sets of 25 repetitions each, three days a week or 11 sessions over four weeks.

Bone density measurements were obtained using DEXA. The HS group BMD at the distal femur decreased 7.7% from day 0. However, the BMD values for HSRT were not significantly different from the control group, indicating that the resistance training protocol was effective in mitigating bone loss during mechanical unloading. Because the distal femur is composed largely cancellous bone, it is comparable to the proximal tibia in the current study, which demonstrated that BMD levels for exercised rats were much higher than those of weight-bearing controls, effectively maintaining bone mass.

The flywheel resistive exercise is a voluntary exercise performed by a conscious animal. The effects of the activated sympathetic nervous system could influence bone health. Flywheel resistance training and the current study's electrical muscle stimulation protocol both attenuate bone loss from cancellous bone sites during hindlimb suspension. However, the previously published flywheel study did not evaluate the effects on bone mechanical properties. It also did not allow for control of the intensity level of the exercise because the exercise is purely voluntary and based on the animal's voluntary participation.

### 5.3.3 *Limb immobilization, mechanical loading, and calcium restriction*

This study evaluated the mechanical properties of immobilized bone in animals fed a calcium-deficient diet. Twenty-eight female Sprague-Dawley rats (five months old) were divided into three groups, control, immobilized, and immobilized with loading. If calcium deficiency is coupled with the effects of disuse, the rate of bone loss is accelerated because of the resulting increase in serum parathyroid hormone (PTH).

Chronically elevated serum PTH can contribute to increased rates of bone resorption and loss of bone mass<sup>29</sup>. Right limbs were immobilized by taping them to the rat's lower torso and received 4-point bending (Figure 36) loading sessions three times a week for six weeks. During the course of the study, the animals did not experience any normal ambulatory loading of the immobilized limb. Mechanical testing of the loaded and unloaded tibiae was performed using three-point bending. Bone densities were determined using DEXA.

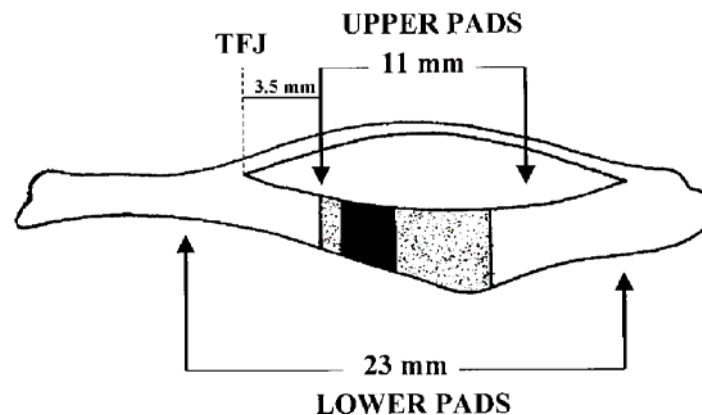


Figure 36: Schematic illustration of in vivo 4-point bending. Loaded region of the tibia extends from 3.5mm to 14.5mm proximal to the tibiofibular junction (TFJ). The lateral surfaces experience tension while the medial surface experiences compression.<sup>29</sup>

After six weeks of immobilization, the immobilized group exhibited lower vBMD and BMC values (10% and 12%, respectively) than those in control rats at the tibial midshaft. The BMC and vBMD of the immobilized + loading group were significantly greater than the immobilized group and equivalent to that of the control group. However, the loading regimen did not change vBMD or BMC at the proximal and distal tibia, so the loading effects were limited to the region that experienced bending during external loading (Figure 36). Because the current study employed a different loading regime that applied loads using the muscle, the results in the cancellous compartment were more significant than for the immobilization study. However, both studies demonstrated positive effects on bone at the tibial midshaft.

The intrinsic mechanical properties did not significantly change with loading or immobilization. However, the maximum loads for both of the immobilized groups were lower than control after six weeks. The loading regimen elevated the maximum load

above that of the immobilized leg. The stiffness of the immobilized limb was 20% lower than control. The immobilized + loading group was not significantly different from either control or the immobilized group. Cross-sectional moment of inertia (CSMI) values for the immobilized and immobilized + loading were 20% and 8% lower, respectively, than control mean values, although these differences were not quite significant.

Because the intrinsic properties did not change with the loading regimen, the tissue-level material properties were not affected. However, the loading protocol attenuated losses in bone structural properties due to disuse and calcium deficiency. Yet this protocol was not physiological, because the loading was applied externally and did not utilize the animal's muscles, even though it allowed the operator to control load levels. The sedation method is similar to muscle stimulation anesthesia, but it does not allow for the multiple physiological effects of an activated sympathetic nervous system.

#### *5.3.4 Muscle stimulation simulated resistive exercise*

A recent study done by the researcher's lab group employed a similar muscle stimulation regime (Alcorn)<sup>19</sup>. However, there were a few parameters in the current study that were changed in order to evaluate the effects on both muscle and bone (both studies are part of a larger experiment that looks at the response of both bone and muscle, but the current study only looked at bone). The starting angle for the foot pedal in Alcorn's study was at a 90 degree angle to the tibial long axis (Figure 37a), whereas the angles were shifted 20 degrees for more plantarflexion in the current study (Figure 37b). In addition to the foot pedal changes, the length of stimulation was increased from 500ms to 1s. The intensity of the contraction was decreased from 120% peak isometric torque to 100%, to ensure that the contraction was not so strong that it damaged muscle.

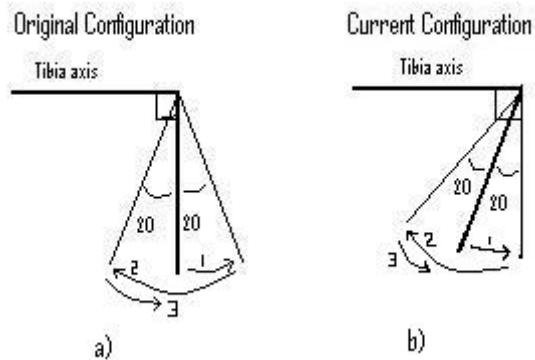


Figure 37: Comparison of foot pedal protocols for the study by Alcorn and the current study. (a) Configuration of the foot pedal for Alcorn's study, with the foot pedal at a 90 degree angle to the axis. (b) Configuration of the foot pedal for the current study, with the foot pedal rotated 20 degrees in dorsiflexion.

The results of Alcorn's study indicated that the exercise countermeasure was effective in mitigating bone loss from disuse. The total BMC at the tibial midshaft was 27% greater for the HU+Ex group as compared to the HU group after 28 days, while the current study demonstrated total BMC levels of 22% higher than that of HU after 28 days. For both studies, the exercise regimen maintained BMC levels with that of CC. For Alcorn's study, the total vBMD at the metaphysis for the exercise group was 11% greater than the HU group, comparing to 16.8% for the current study. The ultimate stress for the HU+Ex group in Alcorn's study was 217% greater than the HU group, as compared to 268% for the current study. The elastic modulus was 440% greater for the exercise group as compared to the HU group, while for the current study, no difference was found.

Similar results were found in the two studies, indicating that the loading intensities were comparable. However, muscle loss was not mitigated for either study<sup>40</sup>. This suggests that a higher intensity regimen might be worth investigating to find a positive effect on muscle.

## 5.4 Conclusion

The density, area, BMC, and intrinsic properties of the proximal tibial metaphysis are decreased by hindlimb suspension. The total vBMD at the proximal tibia decreased 3.0% from day 0 to day 28, which is consistent with previous results in similar studies<sup>19,30</sup>. The addition of a countermeasure proved effective in mitigating the loss and raising vBMD levels well above those of the control group, and improved intrinsic mechanical properties. In addition, the current study demonstrated significantly increased vBMD and BMC levels in the tibial midshaft while exposed to longterm unloading (28 days). Further investigation of the tibial midshaft response merits investigation for future studies. The countermeasure of stimulated resistive exercise proved to be an effective method of preventing loss due to disuse. This is the first study that demonstrates not only mitigation of loss, but also actual gain of bone parameters during hindlimb unloading.

The intrinsic properties of the bone provide a picture of the material's behavior. The countermeasure moderated the negative effect of disuse on mechanical properties and strengthened the bone. Because the ultimate stress of the exercise group was so much higher than the control group, the loading pattern may be greater than normal physiological loads and goes beyond mitigating loss. This indicates that a more optimal loading regime may yet exist that strengthens the bone, maintaining material properties at the control level while still mitigating loss from disuse.

## **6. FUTURE WORK**

### **6.1 Potential muscle problems**

Although the focus of this study was on bone and not muscle, the experience gained with the muscle stimulation protocol provides an opportunity for some observations. One potential concern is that the current muscle stimulation procedure may cause muscle damage. The muscles are harvested at necropsy and should be inspected for damage. The stimulation at 100% peak isometric torque produces a high intensity contraction, so it is worth investigating the muscle for animal welfare reasons. Although mild muscle damage is common after normal resistance training or unaccustomed exercise, it is important to consider whether lower intensity contractions would result in less muscle damage. Finding an optimal loading regime that would have minimal muscle damage would be useful in finding a more physiological level of eccentric contractions.

### **6.2 Varying intensity levels**

A previous study evaluated the osteogenic effect at 120% peak isometric torque<sup>19</sup>. In the current study, the osteogenic effect at 100% peak isometric torque was considered. However, because the foot pedal angles were different in the two studies, the intensities of the two are more comparable. Future considerations would be to determine whether lower stimulation intensity levels would be acceptably osteogenic.

In addition to varying the intensity of the contractions, another useful consideration would be to look at the impact of the starting angle of rotation for the foot pedal during eccentric contractions. Achieving the maximum lengthening of the muscle during contraction would likely produce greater loads on the bone. This should induce an osteogenic response, in addition to a response in the muscle.

### **6.3 Drug and exercise interactions**

The next phase of hindlimb unloading experiments is to incorporate bisphosphonate drugs into the experiment. Bisphosphonates are a class of drugs that inhibit bone resorption. Investigating the osteogenic effects of a bisphosphonate (i.e. alendronate) by itself during disuse should be considered before incorporating the drug

into exercise experiments. The combination of anti-resorption drugs and exercise may help to further attenuate bone loss during disuse.

## REFERENCES

1. Khan K., McKay H., Kannus P., Bailey D., Wark J., and Bennell K. 2001 Physical Activity and Bone Health. Human Kinetics, Champaign, IL, USA.
2. Cowin S.C. 2001 Bone Mechanics Handbook. CRC Press LLC, Boca Raton, FL, USA.
3. Siegel I.M. 1998 All About Bone: An Owner's Manual. Demos Medical Publishing, Inc., New York, NY, USA.
4. Martin R.B., Burr D.B., Sharkey N.A. 1998 Skeletal Tissue Mechanics. Springer-Verlag New York Inc., New York, NY, USA.
5. Lang T., LeBlanc A., Evans H., Lu Y., Genant H., and Yu A. 2004 Cortical and trabecular bone mineral loss from the spine and hip in long-duration spaceflight. *Journal of Bone and Mineral Research*, 19 (6): 1006-1012.
6. Smith S., Wastney M., Morukov B., Larina I., Nyquist L., Abrams S., Taran E., Shih C.Y., Nillen J., Davis-Street J., Rice B., and Lane H. 1998 Calcium metabolism before, during and after a 3 month spaceflight: Kinetic and biochemical changes. Life Sciences Research Laboratories/SD3, NASA Johnson Space Center Houston, TX 77058.
7. Vico L., Novikov V., Very J., and Alexandre C. 1991 Bone histomorphometric comparison of rat tibial metaphysis after 7-day tail suspension vs. 7-day spaceflight. *Aviation, Space and Environmental Medicine*, 1:26-31.
8. Dehority W., Halloran B., Bikle D., Curren T., Kostenuik P., Wronski T., Shen Y., Rabkin B., Bouraoui A., and Morey-Holton E. 1999 Bone and hormonal changes induced by skeletal unloading in the mature male rat. *American Journal of Physiology* 276:62-69.
9. Wolff, Julius 1986 The Laws of Bone Remodeling. Springer-Verlag Berlin Heidelberg, Germany.
10. Frost H. 2003 Update of bone physiology and Wolff's Law for clinicians. *Angle Orthodontist*: 74(1):3-15.
11. LeBlanc A.D., Schneider V.S., Evans H.J., Engelbretson D.A., and Krebs J.M. 1990 Bone mineral loss and recovery after 17 weeks of bed rest. *Journal of Bone and Mineral Research*: 5 (8): 843-850.

12. Shackelford L.C., LeBlanc A.D., Driscoll T.B., Evans H.J., Rianon N.J., Smith S.M., Specter E., Feeback D.L., and Lai D. 2004 Resistance exercise as a countermeasure to disuse-induced bone loss. *Journal of Applied Physiology*: 97:119-1291
13. Rubin, C.; Xu, G.; Judex, S. 2001 The anabolic activity of bone tissue, suppressed by disuse, is normalized by brief exposure to extremely low-magnitude mechanical stimuli. *The FASEB Journal*: 15:2225-2229.
14. Turner C., Akhter M., Raab D., Kimmel D., Recker R. 1991 A noninvasive, *in vivo* model for studying strain adaptive bone modeling. *Bone*: 12:73-79.
15. Keller T., Spengler D., Carter D. 1986 Geometric, elastic, and structural properties of maturing rat femora. *Journal of Orthopaedic Research*: 4:57-67.
16. Robling A., Duijvelaar K., Geevers J., Ohashi N., and Turner C. 2001 Modulation of appositional and longitudinal bone growth in the rat ulna by applied static and dynamic force. *Bone*: 29:105-113.
17. Hubal M., Ingalls C., Allen M., Wenke J., Hogan H.A., and Bloomfield S.A. 2005 Effects of eccentric exercise training on cortical bone and muscle strength in the estrogen-deficient mouse. *Journal of Applied Physiology*: 98:1674-1681.
18. Morgan E., Bayraktar H., and Keaveny T. 2003 Trabecular bone modulus-density relationships depend on anatomic site. *Journal of Biomechanics*: 36: 897-904.
19. Alcorn J.D. 2006 Osteogenic effect of electric muscle stimulation as a countermeasure during hind limb unloading. M.S. Thesis, Texas A&M University.
20. Vico L., Collet P., Guignandon A., Lafage-Proust M., Thomas T., Rehalia M., and Alexandre C. 2000 Effects of long-term microgravity exposure on cancellous and cortical weight-bearing bones of cosmonauts. *The Lancet*: 355: 1607-11.
21. Bloomfield S.A., Allen M.R., Hogan H.A., and Delp M.D. 2002 Site- and compartment-specific changes in bone with hindlimb unloading in mature adult rats. *Bone*: 31(1): 149-157.
22. Hogan H.A., Ruhmann S., Sampson H.W. 2000 The mechanical properties of cancellous bone in the proximal tibia of ovariectomized rats. *Journal of Bone and Mineral Research*: 15(2): 284-292.
23. Carmeliet C., Vico L., and Bouillon R. 2001 Space flight: A challenge for normal bone homeostasis. *Critical Reviews in Eukaryotic Gene Expression*: 11:131-144.
24. Giangregorio L. and Blimkie J. 2002 Skeletal adaptation to alterations in weight-bearing activity. *Sports Medicine*: 32:459-476.

25. Koba S., Yoshida T., Hayashi N. 2006 Differential sympathetic outflow and vasoconstriction responses at kidney and skeletal muscles during fictive locomotion. *American Journal of Physiology*: 290: H861-H868.
26. Wei C.N., Ohiri Y., Tanaka T., Yonemitsu H., and Ueda A. 1998 Does electrical muscle stimulation prevent hindlimb suspension induced bone loss? *Journal of Japanese Physiology*: 48: 33-37.
27. Hsieh Y., Robling A., Ambrosius W., Burr D., and Turner C. 2001 Mechanical loading of diaphyseal bone in vivo: The strain threshold for an osteogenic response varies with location. *Journal of Bone and Mineral Research*: 16(12): 2291-2297.
28. Fluckey J.D., Dupont-Versteegden E.E., Montague D.C., Knox M., Tesch P., Peterson C.A., and Gaddy-Kurten D. 2002 A rat resistance exercise regimen attenuates losses of musculoskeletal mass during hindlimb suspension. *Acta Physiologica Scandinavica*: 176 (4): 293-300.
29. Inman C, Warren G., Hogan H, and Bloomfield S. 1999 Mechanical loading attenuates bone loss due to immobilization and calcium deficiency. *Journal of Applied Physiology*: 87:189-195.
30. Allen M.R., Hogan H.A., Bloomfield S.A. 2006 Differential bone and muscle recovery following hindlimb unloading in skeletally mature male rats. *Journal of Musculoskeletal and Neural Interaction*: 6(3): 217-225.
31. Kohrt W., Bloomfield S., Little K., Nelson M., and Yingling V. 2004 ACSM position stand: Physical activity and bone health. *Medicine and Science in Sports and Exercise*: 36(11):1985-1996.
32. Going S., Lohman T., Houtkooper L., Metcalfe L., Flint-Wagner H., Blew R., Stanford V., Cussler E., Martin J., Teixeira P., Harris M., Milliken L., Figueroa-Galvez A., and Weber J. 2003 Effects of exercise on bone mineral density in calcium-replete postmenopausal women with and without hormone replacement therapy. *Osteoporosis International*: 14:637-643.
33. Morey-Holton E.R., Globus R.K., Kaplansky A., and Durnova G. 2005 The hindlimb unloading rat model: Literature overview, technique update and comparison with space flight data. *Experimentation with Animal Models in Space*: 7-40.
34. Warren G.L., Stallone J.L., and Allen M.R. 2004 Functional recovery of the plantar flexor muscle group after hindlimb unloading in the rat. *European Journal of Applied Physiology*: 93: 130-138.

35. Kanis J.A., World Health Organization. 1994 Assessment of fracture risk and its application to screening for postmenopausal osteoporosis. *Osteoporosis International*: 4:368-381.
36. Allen M.R., Hogan H.A., and Bloomfield S.A. 2006 Differential bone and muscle recovery following hindlimb unloading in skeletally mature male rats. *Journal of Musculoskeletal and Neuronal Interaction*: 6(3): 217-225.
37. St. Vincent's Institute, Australia 2006 Bone, Joint, and Cancer: Research Themes. Available online at [www.svi.edu.au](http://www.svi.edu.au). Accessed June 6, 2007.
38. Robling A.G., Hinant F.M., Burr D.B., Turner C.H. 2002 Improved bone structure and strength after long-term mechanical loading is greatest if loading is separated into short bouts. *Journal of Bone and Mineral Research*: 17(8): 1545-1554.
39. Akhter M., Cullen D., Pedersen E., Kimmel D., and Recker R. 1998 Bone response to in vivo mechanical loading in two breeds of mice. *Calcified Tissue International*: 63: 442-449.
40. Bloomfield S.A, Sumner L.R., Jeffery J.M., Swift J.M., Nilsson M.I., Hogan H.A., Baldwin K.M. 2007 Eccentric-based resistance training during simulated microgravity stimulates gains in tibial bone mineral content but does not mitigate declines in muscle function or mass. NASA Human Research Program Investigators' Workshop, League City, TX. February 12-14, 2007.

## APPENDIX

### A.1 pQCT scan data and mechanical testing data

Table 1: Summary of the tibial metaphysis pQCT results obtained at day 0 and day 28.  
Data are reported in the form of mean  $\pm$  SD.

	Day	BC	CC	HU+Ex	HU
Metaphysis Total vBMD (mg/cm <sup>3</sup> )	0	595.18 $\pm$ 26.58	591.45 $\pm$ 33.38	596.19 $\pm$ 25.46	600.85 $\pm$ 29.37
	28		600.33 $\pm$ 32.20	680.72 $\pm$ 21.29 <sup>a,b,c</sup>	582.86 $\pm$ 32.49
Metaphysis Cancellous vBMD (mg/cm <sup>3</sup> )	0	275.4042 $\pm$ 33.02474	259.26 $\pm$ 48.16	268.19 $\pm$ 25.81	261.27 $\pm$ 30.38
	28		253.06 $\pm$ 30.67	263.75 $\pm$ 37.41	224.18 $\pm$ 30.05
Metaphysis Cortical vBMD (mg/cm <sup>3</sup> )	0	1042.51 $\pm$ 50.15	1036.99 $\pm$ 48.89	1048.49 $\pm$ 37.33	1059.39 $\pm$ 32.95
	28		1067.45 $\pm$ 28.86	1141.43 $\pm$ 27.96 <sup>a,b,c</sup>	1067.92 $\pm$ 45.78
Metaphysis Total BMC (mg)	0	11.63 $\pm$ 0.87	11.91 $\pm$ 1.20	11.70 $\pm$ 0.49	11.49 $\pm$ 0.42
	28		12.17 $\pm$ 1.08	12.46 $\pm$ 0.54 <sup>a,b</sup>	10.22 $\pm$ 0.53 <sup>b,c</sup>
Metaphysis Cancellous BMC (mg)	0	3.16 $\pm$ 0.73	3.03 $\pm$ 0.87	3.06 $\pm$ 0.61	2.86 $\pm$ 0.46
	28		2.96 $\pm$ 0.65	2.48 $\pm$ 0.46 <sup>b</sup>	2.29 $\pm$ 0.43 <sup>b</sup>
Metaphysis Cortical BMC (mg)	0	7.58 $\pm$ 0.67	7.89 $\pm$ 0.53	7.77 $\pm$ 0.49	7.78 $\pm$ 0.35
	28		8.26 $\pm$ 0.39 <sup>a</sup>	8.82 $\pm$ 0.45 <sup>a,b,c</sup>	7.37 $\pm$ 0.49 <sup>b,c</sup>
Metaphysis Total Area (mm <sup>2</sup> )	0	19.59 $\pm$ 1.80	20.21 $\pm$ 2.33	19.66 $\pm$ 1.18	19.19 $\pm$ 1.19
	28		20.36 $\pm$ 2.28	18.31 $\pm$ 0.79 <sup>b,c</sup>	17.61 $\pm$ 1.33 <sup>b,c</sup>
Metaphysis Marrow Area (mm <sup>2</sup> )	0	11.29 $\pm$ 1.47	11.47 $\pm$ 1.84	11.26 $\pm$ 1.26	10.87 $\pm$ 1.07
	28		11.56 $\pm$ 1.79	9.30 $\pm$ 0.73 <sup>b,c</sup>	10.15 $\pm$ 1.19 <sup>c</sup>
Metaphysis Cortical Area (mm <sup>2</sup> )	0	7.27 $\pm$ 0.56	7.62 $\pm$ 0.47	7.41 $\pm$ 0.29	7.35 $\pm$ 0.29
	28		7.75 $\pm$ 0.41 <sup>a</sup>	7.73 $\pm$ 0.23 <sup>a</sup>	6.99 $\pm$ 0.77

*a*, statistical significance when comparing to HU

*b*, statistical significance when compared to day 0

*c*, statistical significance when comparing to CC

Table 2: Summary of tibial midshaft pQCT results obtained at day 0 and day 28. Data are reported in the form of mean  $\pm$  SD.

	Day	BC	CC	HU+Ex	HU
Midshaft Total BMC (mg)	0	7.26 $\pm$ 0.55	7.14 $\pm$ 0.71	7.19 $\pm$ 0.68	7.01 $\pm$ 0.51
	28		7.69 $\pm$ 0.45 <sup>b</sup>	8.29 $\pm$ 0.57 <sup>a,b,c</sup>	7.26 $\pm$ 0.46
Midshaft Cortical BMC (mg)	0	7.96 $\pm$ 0.53	7.93 $\pm$ 0.72	7.92 $\pm$ 0.70	7.75 $\pm$ 0.49
	28		8.40 $\pm$ 0.46 <sup>b</sup>	9.05 $\pm$ 0.58 <sup>a,b,c</sup>	7.97 $\pm$ 0.42
Midshaft Total vBMD (mg/cm <sup>3</sup> )	0	966.13 $\pm$ 35.09	954.28 $\pm$ 43.47	975.47 $\pm$ 23.90	957.95 $\pm$ 34.65
	28		963.50 $\pm$ 42.30	1032.51 $\pm$ 27.21 <sup>a,b,c</sup>	965.33 $\pm$ 35.03
Midshaft Cortical vBMD (mg/cm <sup>3</sup> )	0	1314.18 $\pm$ 13.58	1312.30 $\pm$ 17.62	1316.81 $\pm$ 12.10	1312.88 $\pm$ 13.55
	28		1323.49 $\pm$ 15.26	1335.71 $\pm$ 11.09	1331.23 $\pm$ 12.32
Midshaft Total Area (mm <sup>2</sup> )	0	7.51 $\pm$ 0.50	7.48 $\pm$ 0.62	7.37 $\pm$ 0.66	7.32 $\pm$ 0.46
	28		8.00 $\pm$ 0.60 <sup>b</sup>	8.03 $\pm$ 0.50 <sup>b</sup>	7.52 $\pm$ 0.41
Midshaft Cortical Area (mm <sup>2</sup> )	0	6.06 $\pm$ 0.36	6.04 $\pm$ 0.51	6.01 $\pm$ 0.52	5.90 $\pm$ 0.37
	28		6.35 $\pm$ 0.36 <sup>b</sup>	6.77 $\pm$ 0.42 <sup>a,b,c</sup>	5.98 $\pm$ 0.32 <sup>c</sup>
Cortical shell thickness (mm)	0	0.87 $\pm$ 0.04	0.87 $\pm$ 0.06	0.87 $\pm$ 0.04	0.86 $\pm$ 0.05
	28		0.88 $\pm$ 0.05	0.97 $\pm$ 0.04 <sup>a,b,c</sup>	0.85 $\pm$ 0.04

*a*, statistical significance when comparing to HU  
*b*, statistical significance when compared to day 0  
*c*, statistical significance when comparing to CC

Table 3: Summary of mechanical testing data and body weights.

	Day	BC	CC	HU+Ex	HU
Elastic Modulus (MPa)	0	14.61 $\pm$ 15.73			
	28		17.58 $\pm$ 29.66	14.98 $\pm$ 17.22	11.85 $\pm$ 17.23
Ultimate Stress (MPa)	0	1.01 $\pm$ 0.71			
	28		0.83 $\pm$ 0.59	2.28 $\pm$ 1.48 <sup>a,c</sup>	0.62 $\pm$ 0.53
Body Weight (g)	0	416.25 $\pm$ 21.79	427.08 $\pm$ 30.25	423.08 $\pm$ 29.18	415.75 $\pm$ 21.36
	28		475.50 $\pm$ 34.10	388.25 $\pm$ 14.80 <sup>a,c</sup>	415.92 $\pm$ 18.20 <sup>b,c</sup>

*a*, statistical significance when comparing to HU  
*b*, statistical significance when compared to day 0  
*c*, statistical significance when comparing to CC

Table 4: Number of animals per group

Group	# of animals
Baseline control (BC)	11
Cage (weight-bearing) control (CC)	12
Hindlimb unloaded (HU)	12
Hindlimb unloaded + exercise (HU+Ex)	10

## A.2 Electric muscle stimulation data

Table 5: Voltage (V) for peak isometric torque at 175 Hz (used at each training session).

	1	2	3	4	5	6	7	8	9	10	11	12	13	14
<b>1606</b>	11	5	5	9	5	5	6	7	6	9	5	11	5	
<b>1610</b>	5	5	7	10	5	6	4	5	4	6	5	5	4	
<b>1611</b>	5	6	5	4	4	6	6	5	4	4	12	4	4	
<b>1613</b>	5	4	6	5	3	5	8	4	6		11	5	4	
<b>1617</b>	4	6	10	5	6	5	5	5	4	9	5	7		
<b>1621</b>	5	13	9	5	4	5	3	5	9	10	7	6		
<b>1635</b>	7	15	7	14	8	8	5	6	8	5	7	13	11	8
<b>1636</b>	8	8	8	11	4	4	11	11	8	6	8	1	14	13
<b>1640</b>	6	12	7	8	10	8	7	13	9	5	6	6	8	13
<b>1643</b>	8	8	8	6	5	5	9	6	7	9	14	6	12	10

Table 6: Peak isometric torque at 175 Hz (used at each training session).

	1	2	3	4	5	6	7	8	9	10	11	12	13	14
<b>1606</b>	.273	.239	.238	.228	.235	.224	.242	.243	.225	.241	.231	.251	.238	
<b>1610</b>	.279	.244	.29	.256	.244	.210	.221	.210	.210	.237	.220	.227	.234	
<b>1611</b>	.254	.237	.229	.225	.264	.221	.231	.241	.223	.259	.264	.253	.217	
<b>1613</b>	.253	.230	.242	.226	.215	.230	.211	.236	.237	.252	.269	.261	.224	
<b>1617</b>	.278	.232	.240	.228	.233	.230	.231	.250	.247	.274	.266	.227		
<b>1621</b>	.290	.248	.250	.244	.234	.265	.312	.263	.239	.254	.256	.250		
<b>1635</b>	.285	.264	.284	.215	.203	.202	.215	.221	.242	.246	.249	.263	.238	.251
<b>1636</b>	.271	.268	.261	.259	.239	.249	.252	.249	.261	.245	.240	.250	.245	.232
<b>1640</b>	.238	.188	.206	.216	.207	.222	.208	.192	.221	.232	.204	.202	.212	.224
<b>1643</b>	.290	.275	.292	.282	.278	.299	.293	.272	.289	.246	.225	.208	.208	.205



Table 9: Thickness for specimens (NE=no epiphysis; dimensions in mm)

Rat #	Epiphysis	Specimen	Rat #	Epiphysis	Specimen	Rat #	Epiphysis	Specimen
1435L	4.04	1.90	1615R	4.06	1.74	1633L	3.58	2.06
1435R	3.63	1.98	1616L	4.05	1.93	1633R	3.60	1.97
1600L	4.13	1.90	1616R	NE	1.99	1634L	3.89	1.93
1600R	4.41	2.21	1617L	3.60	1.80	1634R	4.44	2.02
1601L	4.21	1.84	1617R	4.12	1.74	1635L	4.08	1.87
1601R	3.86	2.07	1618L	4.15	1.88	1635R	4.35	1.86
1602L	3.96	1.95	1618R	3.72	1.60	1636L	3.76	1.94
1602R	3.43	1.92	1619L	4.26	1.94	1636R	4.37	1.93
1603L	3.67	1.94	1619R	4.06	1.62	1637L	4.18	2.05
1603R	4.07	2.01	1620L	3.60	1.98	1637R	3.76	1.97
1604L	3.46	1.95	1620R	4.04	1.98	1638L	4.30	1.89
1604R	4.05	3.86	1621L	3.72	1.93	1638R	3.98	1.88
1605L	4.29	1.78	1621R	4.28	1.87	1639L	5.05	2.00
1605R	4.25	1.84	1622L	3.85	1.95	1639R	4.32	1.89
1606L	4.26	2.06	1622R	3.99	1.82	1640L	5.21	1.94
1606R	4.48	2.04	1623L	3.79	1.98	1640R	4.44	2.15
1607L	4.73	1.94	1623R	NE	1.98	1641L	4.14	1.93
1607R	4.12	1.92	1625L	3.97	1.85	1641R	4.52	2.01
1608L	4.72	1.82	1625R	4.29	2.00	1642L	3.85	2.02
1608R	3.89	2.08	1627L	5.09	1.94	1642R	4.12	1.92
1609L	3.73	2.00	1627R	4.65	1.98	1643L	4.18	2.00
1609R	3.64	1.89	1628L	4.75	2.04	1643R	4.30	1.90
1610L	3.66	1.98	1628R	4.89	1.91	1644L	broken	broken
1610R	3.99	1.85	1629L	4.41	1.99	1644R	4.87	1.69
1611L	3.60	1.89	1629R	5.19	1.98	1645L	3.64	1.94
1611R	4.12	1.83	1630L	4.86	2.01	1645R	4.02	1.94
1612L	3.76	1.94	1630R	4.34	1.96	1646L	4.23	1.89
1612R	NE	1.99	1631L	4.14	1.92	1646R	3.99	1.92
1613L	4.01	2.07	1631R	4.36	1.77	1647L	3.82	1.93
1613R	3.89	1.89	1632L	5.41	2.03	1647R	3.36	1.94
1615L	3.67	1.93	1632R	4.80	1.85			

**VITA**

Lindsay Rebecca Sumner received her Bachelor of Science degree in Biomedical Engineering from Texas A&M University in May 2005. She entered the Mechanical Engineering program at Texas A&M University in January 2006 and received her Master of Science degree in August 2007. Her research interests include bone and tissue mechanics.

Lindsay R. Sumner

Department of Mechanical Engineering

Attn: Harry A. Hogan

3123 TAMU

College Station, TX 77843-3123